Systematic visualisation of molecular QTLs reveals variant mechanisms at GWAS loci

Nurlan Kerimov[1,2], Ralf Tambets[1], James D. Hayhurst[2,3], Ida Rahu[1], Peep Kolberg[1], Uku Raudvere[1], Ivan Kuzmin[1], Anshika Chowdhary[4], Andreas Vija[1], Hans J. Teras[1], Masahiro Kanai[6,7,8], Jacob Ulirsch[6,7,8], Mina Ryten[9], John Hardy[9], Sebastian Guelfi[9], Daniah Trabzuni[9], Sarah Kim-Hellmuth[4,5], Will Rayner[4], Hilary Finucane[6,7,8], Hedi Peterson[1], Abayomi Mosaku[2,3], Helen Parkinson[2,3], Kaur Alasoo[1,2]

[1]Institute of Computer Science, University of Tartu, Tartu, 51009, Estonia
[2]Open Targets, South Building, Wellcome Genome Campus, Hinxton, Cambridge CB10 1SD, UK
[3]European Molecular Biology Laboratory, European Bioinformatics Institute, Wellcome Genome Campus, Hinxton, Cambridge CB10 1SD, UK
[4]Institute of Translational Genomics, Helmholtz Munich, Neuherberg, Germany
[5]Department of Pediatrics, Dr. von Hauner Children's Hospital, University Hospital LMU Munich, Munich, Germany
[6]Analytic and Translational Genetics Unit, Massachusetts General Hospital, Boston, MA, USA
[7]Program in Medical and Population Genetics, Broad Institute of MIT and Harvard, Cambridge, MA, USA
[8]Stanley Center for Psychiatric Research, Broad Institute of MIT and Harvard, Cambridge, MA, USA
[9]Department of Genetics and Genomic Medicine, Great Ormond Street Institute of Child Health, University College London, London
Correspondence should be addressed to K.A. (kaur.alasoo@ut.ee)

Abstract

Splicing quantitative trait loci (QTLs) have been implicated as a common mechanism underlying complex trait associations. However, utilising splicing QTLs in target discovery and prioritisation has been challenging due to extensive data normalisation which often renders the direction of the genetic effect as well as its magnitude difficult to interpret. This is further complicated by the fact that strong expression QTLs often manifest as weak splicing QTLs and vice versa, making it difficult to uniquely identify the underlying molecular mechanism at each locus. We find that these ambiguities can be mitigated by visualising the association between the genotype and average RNA sequencing read coverage in the region. Here, we generate these QTL coverage plots for 1.7 million molecular QTL associations in the eQTL Catalogue identified with five quantification methods. We illustrate the utility of these QTL coverage plots by performing colocalisation between vitamin D levels in the UK Biobank and all molecular QTLs in the eQTL Catalogue. We find that while visually confirmed splicing QTLs explain just 6/53 of the colocalising signals, they are significantly less pleiotropic than eQTLs and identify a prioritised causal gene in 4/6 cases. All our association summary statistics and QTL coverage plots are freely available at https://www.ebi.ac.uk/eqtl/.

Introduction

Most genetic variants associated with complex traits are in the non-coding regions of the genome (Maurano et al., 2012). More than a decade of molecular quantitative trait locus (QTL) studies has revealed that these variants regulate either the expression level (Kerimov et al., 2021; The GTEx Consortium, 2020), splicing (Li et al., 2016), promoter usage (Alasoo et al., 2019; Garieri et al., 2017) or alternative polyadenylation (Mittleman et al., 2020; Yoon et al., 2012) of their target genes. Although the eQTL Catalogue has contained transcript-level QTL summary statistics from the beginning, characterising the exact mechanism of action of each molecular QTL has remained challenging due to considerable overlap between QTLs detected by different RNA-seq quantification methods (Kerimov et al., 2021), technical biases in read alignment (van de Geijn et al., 2015), and a large number of alternative transcripts or splice junctions to be considered for each gene. Furthermore, because the usage of each transcript or splice junction is quantified relative to all other transcripts, the magnitude and direction of the genetic effect, the part of the gene affected, as well as the absolute expression of the affected transcript is often difficult to assess from summary statistics alone.

This ambiguity can be reduced by visualising the change in the average RNA-seq read coverage in the gene region associated with each additional copy of the alternative allele. We and other have used these QTL coverage plots to characterise chromatin QTLs (Alasoo et al., 2018; Degner et al., 2012; Kumasaka et al., 2018) as well as to confirm promoter usage and splicing QTLs (Alasoo et al., 2019). However, previous studies have visualised individual molecular QTLs in a setting where access to individual-level genotype and read coverage data is available. It has not been done systematically in large molecular QTL compendia such as the GTEx project (The GTEx Consortium, 2020) and the eQTL Catalogue, because in a naive implementation the read coverage stratification by genotype needs to be performed separately for each significant genetic variant and molecular trait pair of interest. Since transcript and exon-level analyses profile hundreds of thousands of correlated molecular traits in a single dataset, this means that the number of QTL coverage plots required can quickly become intractable.

In this update to the eQTL Catalogue, we present an approach to generate QTL coverage plots for all independent genetic signals and their associated molecular traits. First, we have updated our data processing workflows to improve promoter usage and splicing QTL discovery and to generate read coverage signals for all 25,724 RNA-seq samples. We have also adopted fine-mapping-based filtering to identify all independent genetic signals and associated molecular traits for each gene while reducing the size of the summary statistics files by 98%. Finally, to support new colocalisation methods that can account for multiple independent causal variants (Wallace, 2021), we have computed signal-level log Bayes factors for all independent signals (Wang et al., 2020). This approach has enabled us to predefine tag variants for all independent genetic associations identified in 127 eQTL datasets and generate QTL coverage plots that can be used to interpret almost all colocalising signals detected in the eQTL Catalogue.

Results

Updates to the eQTL Catalogue resource

The aim of the eQTL Catalogue is to provide a public resource of uniformly processed molecular QTL summary statistics and continuously update this resource as new studies, reference annotations and quantification methods become available. Here, we present the updates to the eQTL Catalogue release 6 that we have made since the publication of the original paper (release 3).

Newly added datasets

We have added nine new RNA-seq studies and one microarray study to the eQTL Catalogue. This has increased the total number of studies in the resource to 31, the total number of datasets to 127 and the cumulative number of donors and samples to 7,526 and 30,602, respectively (Figure 1A). Newly added datasets include additional datasets from tissues and cell types already present in the eQTL Catalogue (e.g. various brain regions (Guelfi et al., 2020; Hoffman et al., 2019), immune cells (Bossini-Castillo et al., 2022; Gilchrist et al., 2022; Kim-Hellmuth et al., 2017; Theusch et al., 2020) and induced pluripotent stem cells (DeBoever et al., 2017; Pashos et al., 2017)) as well as previously missing microglia (Young et al., 2021), placenta (Peng et al., 2018), hepatocytes (Pashos et al., 2017), and cartilage and synovium tissues (Steinberg et al., 2021). Complete summary of the datasets present in the eQTL Catalogue is shown in Supplementary Table 1.

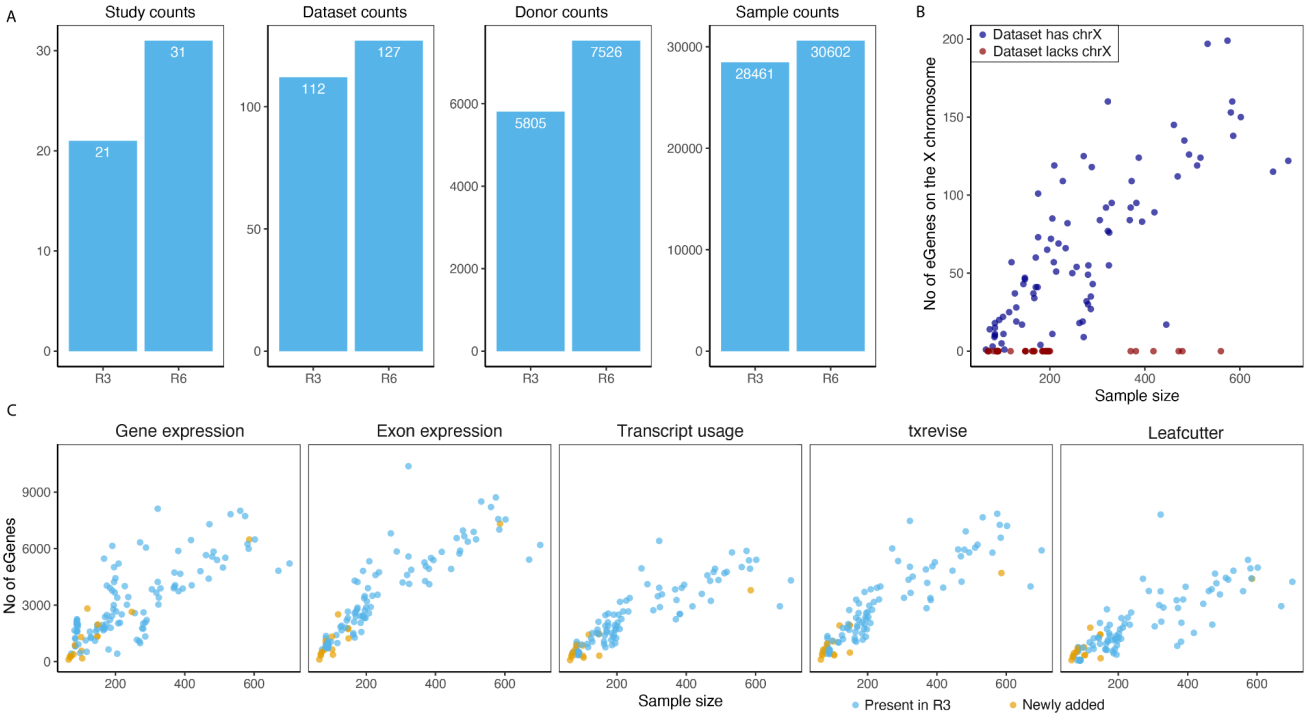

Figure 1. Uniform re-processing of all datasets. (**A**), The number of studies, datasets, donors, and samples in the previous publication (R3) and current version of the eQTL Catalogue (R6). **(B**), Number of genes with at least one significant eQTL ('eGenes') on the X chromosome as a function of dataset sample size. Red points indicate datasets for which the X chromosome genotypes were unavailable. (**C),** The number of eGenes identified in each dataset for the five molecular traits (gene expression, exon expression, transcript usage, txrevise event usage, and Leafcutter splice-junction usage). Datasets newly added since release 3 have been highlighted.

Imputation of the X chromosome genotypes

In addition to integrating new datasets, we also made two major changes to our genotype imputation workflow. First, we migrated to the new 1000 Genomes 30x of GRCh38 reference panel (Byrska-Bishop et al., 2022). This allowed us to impute genotypes directly to the GRCh38 build and avoid errors caused by the genomic coordinate lift over process. Secondly, our imputation workflow now also supports the X chromosome. As a result, summary statistics for 18 of the 31 studies now also contain variants from the X chromosome. Across these 18 datasets, we detected at least one significant eQTL (FDR <1%) for 853 unique genes on the X chromosome (Figure 1B). These X chromosome eQTLs account for ~1.6% of all significant eQTLs (FDR <= 1%). Ten of the other 13 studies are missing the X chromosome QTLs because X chromosome genotypes were not deposited with data. Exceptions are male only studies (n = 3) that did not pass our genotype QC criteria (Supplementary Table 2).

Improved quantification of splicing and promoter usage QTLs

The previous release of the eQTL Catalogue included four molecular trait quantification methods to measure transcriptional changes from RNA-seq data: gene expression (ge), exon expression (exon), transcript usage (tx) and transcriptional event usage (txrevise). In addition to these four, we have now also implemented LeafCutter (Li et al., 2018) to directly quantify the usage of splice junctions (Supplementary Figure 1). We have also augmented the txrevise promoter annotations with experimentally determined promoters from the FANTOM5 project (Vija and Alasoo, 2022). Finally, we have updated the reference transcriptome annotations to Ensembl version 105 and GENCODE version 39. We observed a clear linear relationship between the number of significant associations detected with each quantification method and the dataset sample size, with gene expression, exon expression and txrevise detecting, on average, slightly more associations than transcript usage and Leafcutter (Figure 1C).

Fine-mapping-based filtering of transcript-level summary statistics

A major challenge in working with exon- and transcript-level (transcript usage, txrevise, leafcutter) associations is the large number of correlated traits being tested that result in very large summary statistics files. For example, typical summary statistics for exon and txrevise QTLs are 15-20 times larger than the corresponding files for gene expression QTLs. In addition to complicating our data release and archival procedures, these large file sizes meant that performing comprehensive colocalisation analysis against the eQTL Catalogue required the downloading and processing of >15Tb of data. To reduce the size of these files, we have now

implemented fine-mapping-based filtering. Briefly, we are using fine mapped credible sets to identify all independent signals at the gene level. We then filter the summary statistics files to only retain the most strongly associated molecular trait (exon, transcript, txrevise event or Leafcutter splice junction) for each signal. This filtering reduces the size of the summary statistics files for those quantification methods by ~98% while retaining almost all significant associations for colocalisation purposes. Reducing the size of the univariate summary statistics files has also allowed us to export SuSiE log Bayes factors for each fine mapped signal and all tested variants (Wang et al., 2020). As illustrated below, these log Bayes factors can be directly used in the new coloc.susie method to perform colocalisation analysis between all pairs of independent signals (Wallace, 2021).

Visualisation of transcript-level associations

Another benefit of fine-mapping-based filtering is that we now have a tractable set of independent lead variants and associated molecular traits across all datasets and quantification methods that we can visualise using static QTL coverage plots. These plots display normalised RNA-seq read coverage across all exons of the gene (Figure 2A), exon-level QTL effect sizes and standard errors (Figure 2B), as well as the alternative transcripts or splice junctions used in association testing (Figure 2C). As an example, we are highlighting the association between chr11_14855172_G_A and alternative splicing of exon four of the *CYP2R1* gene (Figure 2). The static QTL coverage plots for all 1,716,482 independent signals are now available via the eQTL Catalogue FTP server.

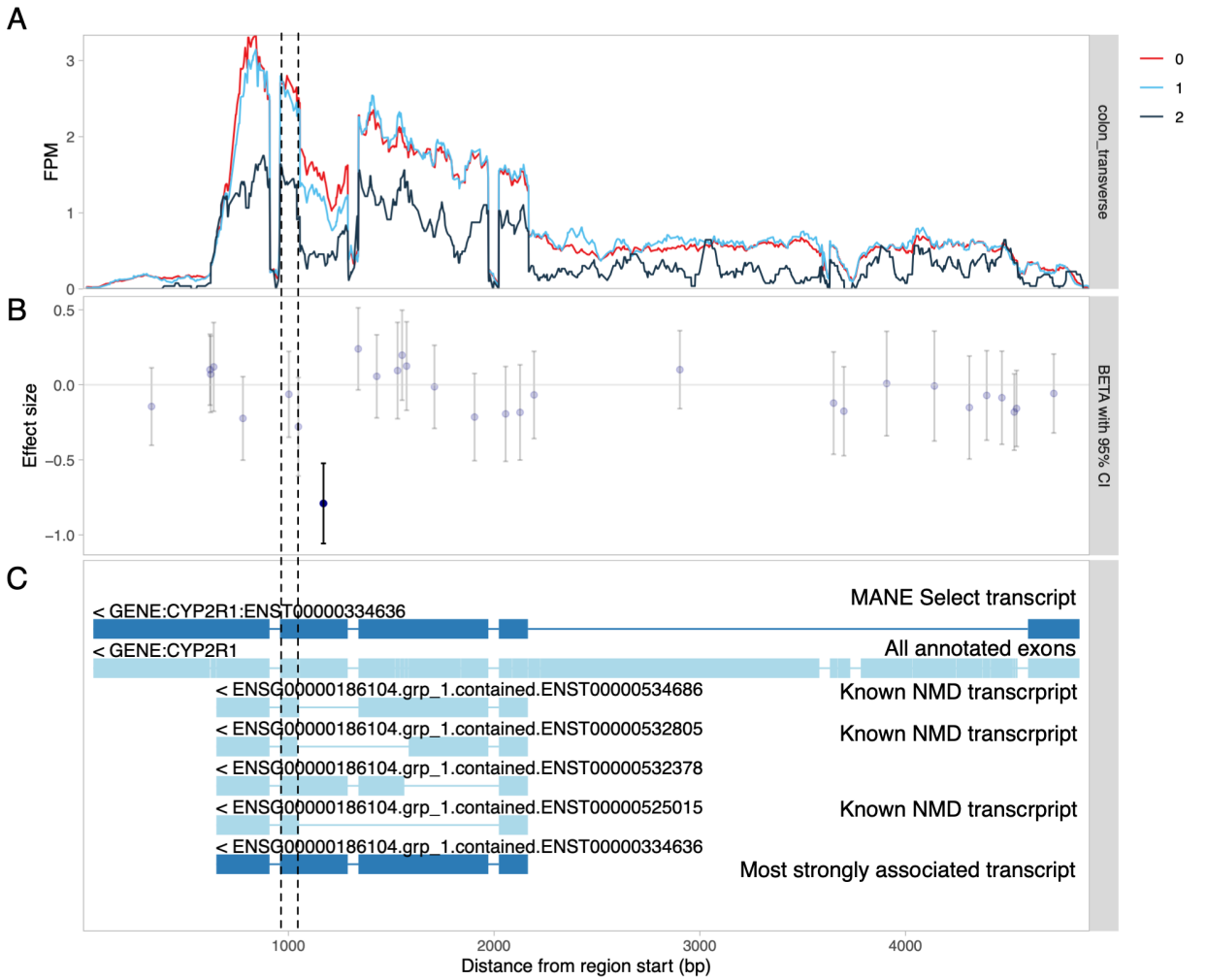

Figure 2. Visualisation of a splicing QTL detected in the *CYP2R1* gene. (**A**) RNA-seq read coverage across the *CYP2R1* gene in GTEx transverse colon tissue stratified by the genotype of the lead sQTL variant (chr11_14855172_G_A). All introns have been shortened to 50 nt with wiggleplotr (Alasoo, 2017) to make variation in exonic read coverage easier to see. (**B**) Effect sizes and 95% confidence intervals of the lead sQTL variant on the expression level of individual exons (or exonic parts) of *CYP2R1*. Associations significant at FDR <= 1% are shown in dark blue. (**C**) The top two rows show the MANE Select (Morales et al., 2022) reference transcript and all annotated exons of *CYP2R1*, respectively. The remaining rows show the txrevise (Alasoo et al., 2019) event annotations used for sQTL mapping. The short version of exon 4 (between dashed lines) is only present in annotated nonsense-mediated decay (NMD) transcripts.

Case study: target gene prioritisation for vitamin D GWAS

To test the utility of the new QTL coverage plots, we performed a proof-of-concept colocalisation analysis between all molecular traits in the eQTL Catalogue and vitamin D levels in the UK Biobank. We chose this phenotype, because the vitamin D biosynthesis pathway is well understood and many causal genes underlying GWAS associations for vitamin D are already

known (Hyppönen et al., 2022; Manousaki et al., 2020). At a stringent threshold of PP4 > 0.9, we found that 53/83 signals from 34/48 regions colocalised with 81 protein coding genes (Figure 3A). Although colocalisation with total gene expression was most common, there was considerable overlap between colocalisations detected with the five different quantification methods (Figure 3A).

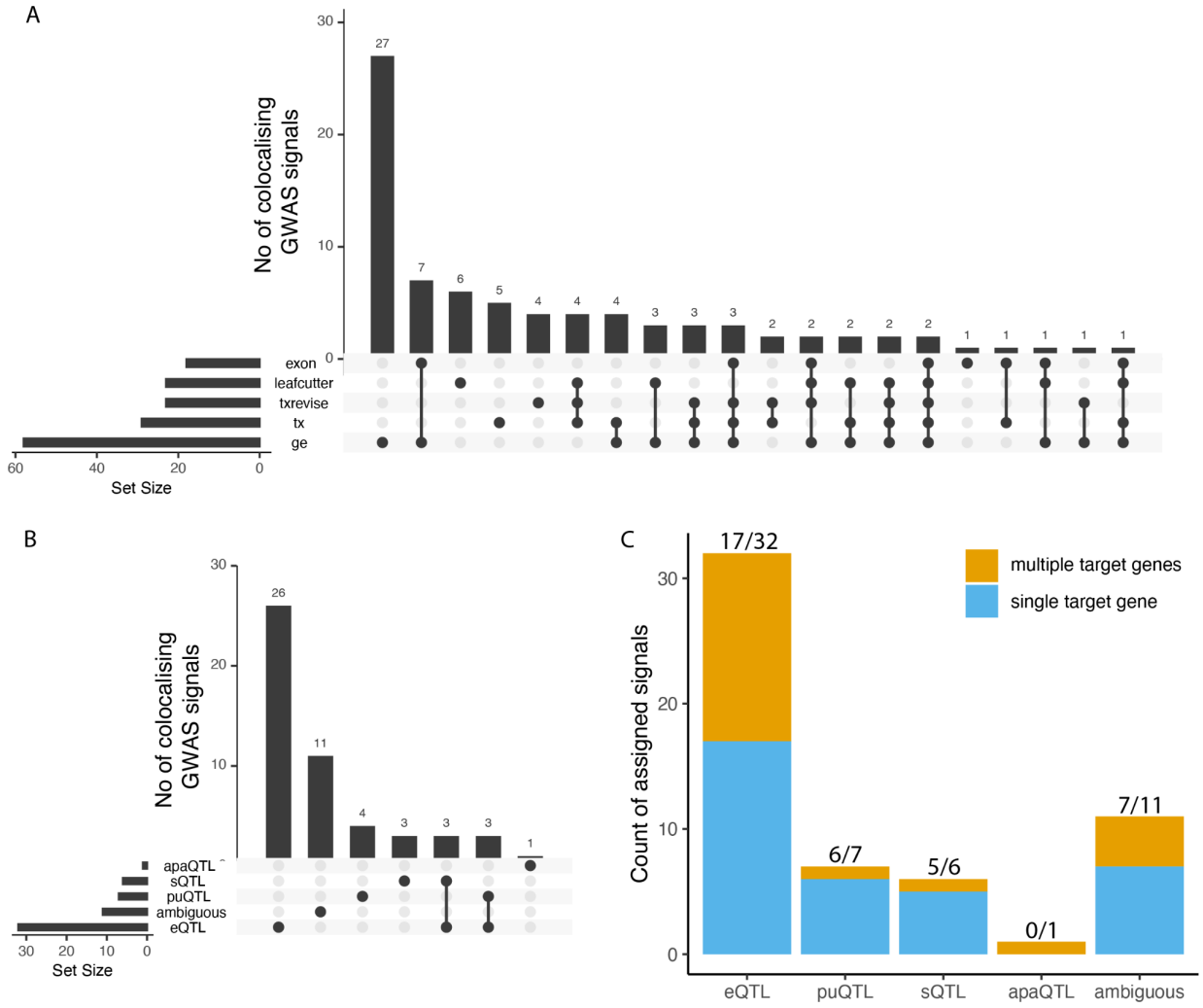

Figure 3. Sharing of significantly colocalised signals with vitamin D (**A**) Number of colocalised signals detected by the different molecular QTL quantification methods and sharing between them. (**B**) Number of colocalised signals assigned to empirical functional consequence (eQTL, sQTL, puQTL, apaQTL or ambiguous) and sharing structure between them. (**C**) Number of independent colocalised signals associated with either a single target gene or multiple target genes in each functional consequences group. eQTL - expression QTL, sQTL - splicing QTL, puQTL - promoter usage QTL, apaQTL - alternative polyadenylation QTL.

We extracted QTL coverage plots for all 816 colocalising molecular QTL signals. We then manually reviewed the plots to classify each signal into one of five categories: expression QTLs, promoter usage QTLs (puQTLs), splicing QTLs (sQTLs), alternative polyadenylation QTLs

(apaQTLs) and ambiguous (Figure 3B). As an example, we detected a splicing QTL affecting the length of exon 4 of *CYP2R1* (Figure 2). *CYP2R1* is highly likely to be the causal gene at this locus as it codes the Cytochrome P450 2R1 microsomal vitamin D 25-hydroxylase (Cheng et al., 2003). We found that although transcript-level methods (tx, txrevise and leafcutter) detected at least one colocalisation for 37/53 independent signals, only 14 of those (7 puQTLs, 6 sQTLs and 1 apaQTL) could be classified as primary transcript-level QTLs (Figure 3B). Other 23 cases were either ambiguous or could be better explained by strong primary eQTL effects that led to small downstream changes in splicing or transcript usage (Supplementary Table 3).

Even though Leafcutter detected all seven visually confirmed sQTLs and 5/7 puQTLs, it also detected 11 additional signals, nine of which would be better explained by a strong eQTL effects (e.g. *CELSR2* eQTL at the *SORT1* locus (Supplementary Figure 2)). Thus, the fact that colocalisation is detected by one of the transcript-level methods (tx, txrevise or leafcutter) does not reliably indicate that the underlying signal is driven by a splicing mechanism. The visualisations also helped us to detect three likely cases of reference mapping bias at the *DHCR7*, *NUDT9* and *JUND* genes (Supplementary Figures 3-5). For discussion of why we opted not to correct for reference mapping bias during molecular trait quantification, see Supplementary Note.

We also noticed that 15/32 confirmed eQTL colocalised with more than one gene (Figure 3C). In contrast, only one of seven puQTLs and one of six sQTLs colocalised with multiple genes, suggesting that sQTLs and puQTLs might be less pleiotropic than eQTLs. To evaluate if lower pleiotropy also translated into more accurate causal gene prioritisation, we manually reviewed all of the 53 GWAS signals to identify the most likely causal genes. We integrated information about missense variant associations, gene presence in the vitamin D synthesis pathway and other literature evidence to prioritise the most likely causal gene for 28/53 GWAS signals (Supplementary Table 3). For four of the six sQTL signals, the colocalising gene overlapped the prioritised causal gene (*CYP2R1*, *HAL*, *GC* and *SDR42E1)* and for two signals we could not prioritise the causal gene. For eQTLs, we prioritise the most likely causal gene at 19/32 loci. In 11/19 cases (3 shared with sQTLs, Figure 3B) the colocalising eQTL genes completely overlapped the prioritised genes. In four cases the prioritised gene (*SORT1*, *FLG*, *HAL*, *CETP*) was one of multiple co-localizing genes. Finally, at four additional signals, the prioritised gene was different from the one that had eQTL colocalisation evidence (Supplementary Table 3). Interestingly, in three of the four cases the GWAS lead variant was a missense (*SEC23A*, *PLA2G3*) or a synonymous variant (*CYP2R1)* in the prioritised gene. While the number of loci observed here is small, these results suggest that while visually confirmed sQTLs colocalise with a smaller fraction of GWAS loci than eQTLs (6 vs 32), they are also less pleiotropic and thus more likely to identify the correct causal gene.

Discussion

We have made three major changes to the eQTL Catalogue in release 6. First, we have integrated data from ten additional eQTL studies bringing the total number of unique eQTL datasets to 127. These datasets contain uniformly processed results from 30,602 samples from 7,526 individuals. We have also updated our genotype imputation, RNA-seq analysis and QTL mapping workflows to add support for the X chromosome, added Leafcutter as a splicing quantification method and added support for fine mapping-based colocalisation analysis with coloc.susie (Wallace, 2021). Finally, we have developed static QTL coverage plots to visualise molecular QTL associations at the level of RNA-seq read alignments. All our results and data are available on the eQTL Catalogue FTP server and REST API.

To quantify the impact of these updates, we performed colocalisation between all molecular QTLs present in the eQTL Catalogue and fine mapped GWAS signals for plasma vitamin D levels in the UK Biobank (Kanai et al., 2021). The QTL coverage plots allowed us to assign an empirical functional consequence (eQTL, sQTL, puQTL, apaQTL) for 42/53 colocalising loci while 11 remained ambiguous. This revealed that while primary sQTLs explained fewer GWAS signals than eQTLs, they also appeared to be less pleiotropic and more likely to identify the correct target genes. A limitation of our approach is that we used manual visual inspection to assign mechanisms to different types of molecular QTLs. Although we tried to be careful, there is a small risk that this approach could have introduced inadvertent confirmation bias (e.g. classifying less pleiotropic loci as sQTLs). We expect that it might be possible to automate this classification in the future by machine learning approaches that consider variant-level annotations such as splicing scores (Jaganathan et al., 2019; Zeng and Li, 2022) or distance to genomic features.

We also observed that while most GWAS signals colocalised with an eQTL, approximately ~50% of the eQTL colocalisations prioritised more than one gene. Similarly in 4/19 cases, the colocalising gene was different from the manually prioritised causal gene. This agrees with multiple previous observations that eQTL colocalisation alone often achieves low precision in causal gene identification (Mountjoy et al., 2021; Nasser et al., 2021). This does not seem to be a simple artefact of colocalisation analysis as CRISPR experiments have also revealed that targeting a single enhancer often regulates the expression of multiple target genes (Engreitz et al., 2016; Fulco et al., 2019; Kasela et al., 2021). We believe that while eQTL colocalisation can sometimes reveal trait-relevant tissues or cell types, target gene identification requires integration of multiple strands of evidence. Considering variants with potentially less pleiotropic effects such as missense and splice variants can also be helpful.

The systematic re-analysis and visualisation of molecular QTLs presented here would not have been possible without the researchers of the 31 original studies making their individual-level gene expression and genotype data available for qualified researchers. We are committed to sharing all summary statistics and fine mapping results openly and will seek to continuously integrate new eQTL datasets as they become available. We are also working on making the static QTL coverage plots available via an API and an interactive web interface.

Methods

Data access and informed consent

For all newly added datasets, we applied for access via the relevant Data Access Committees. The database accessions and contact details of the individual Data Access Committees can be found on the eQTL Catalogue website (http://www.ebi.ac.uk/eqtl/Studies/). In our applications, we explained the project and our intent to share the association summary statistics publicly. Ethical approval for the project was obtained from the Research Ethics Committee of the University of Tartu (approval 287/T-14).

Genotype data

Pre-imputation quality control. We lifted coordinates of the genotyped variants to the GRCh38 build with CrossMap v0.4.1 (Zhao et al., 2014). We aligned the strands of the genotyped variants to the 1000 Genomes 30x on GRCh38 reference panel (Byrska-Bishop et al., 2022) using Genotype Harmonizer (Deelen et al., 2014). We excluded genetic variants with Hardy-Weinberg p-value < 10^{-6}, missingness > 0.05 and minor allele frequency < 0.01 from further analysis. On the X chromosome, we applied the QC filters to female samples only and then retained the same variants also in the male samples. We also excluded samples with more than 5% of their genotypes missing.

Genotype imputation and quality control. We pre-phased and imputed the microarray genotypes to the 1000 Genomes 30x on GRCh38 reference panel (Byrska-Bishop et al., 2022) using Eagle v2.4.1 (Loh et al., 2016) and Minimac4 (Das et al., 2016). On the X chromosome, we performed imputation separately for variants located in the pseudoautosomal (PAR) and non-PAR regions. After imputation, we multiplied male genotype dosage in the non-PAR region by two to ensure that it is on the same scale with the female genotypes. We used bcftools v1.9.0 to exclude variants with minor allele frequency (MAF) < 0.01 and imputation quality score R2 < 0.4 from downstream analysis. The genotype imputation and quality control steps are implemented in eQTL-Catalogue/genimpute (v22.01.1) workflow available from GitHub.

We aligned the low-coverage whole genome sequencing (WGS) data from the BLUEPRINT project to the GRCh38 reference genome with bwa v0.7.17 (Li, 2013) and performed imputation to the 1000 Genomes 30x on GRCh38 reference panel using GLIMPSE v1.1.1 (Rubinacci et al., 2021). The low-coverage WGS genotype imputation workflow is available from GitHub: https://github.com/peepkolberg/glimpse.

Phenotype data

Studies. eQTL Catalogue release 6 contains phenotype data from the following 25 RNA-seq: ROSMAP (Ng et al., 2017), BrainSeq (Jaffe et al., 2018), TwinsUK (Buil et al., 2015), FUSION (Taylor et al., 2019), BLUEPRINT (Chen et al., 2016; Kundu et al., 2020), Quach_2016 (Quach

et al., 2016), Schmiedel_2018 (Schmiedel et al., 2018), GENCORD (Gutierrez-Arcelus et al., 2013), GEUVADIS (Lappalainen et al., 2013), Alasoo_2018 (Alasoo et al., 2018), Nedelec_2016 (Nédélec et al., 2016), Lepik_2017 (Lepik et al., 2017), HipSci (Kilpinen et al., 2017), van_de_Bunt_2015 (van de Bunt et al., 2015), Schwartzentruber_2018 (Schwartzentruber et al., 2018), GTEx v8 (The GTEx Consortium, 2020), CAP (Theusch et al., 2020), Peng_2018 (Peng et al., 2018), PhLiPS (Pashos et al., 2017), iPSCORE (Panopoulos et al., 2017), CommonMind (Hoffman et al., 2019), Braineac2 (Guelfi et al., 2020), Steinberg_2020 (Steinberg et al., 2021), Young_2019 (Young et al., 2021) , Bossini-Castillo_2019 (Bossini-Castillo et al., 2022). It also contains data from the following 7 microarray studies: CEDAR (Momozawa et al., 2018), Fairfax_2012 (Fairfax et al., 2012), Fairfax_2014 (Fairfax et al., 2014), Kasela_2017 (Kasela et al., 2017), Naranbhai_2015 (Naranbhai et al., 2015), Kim-Hellmuth_2017 (Kim-Hellmuth et al., 2017) and Gilchrist_2021 (Gilchrist et al., 2022).

Quantification. We quantified transcription at five different levels: (1) gene expression, (2) exon expression, (3) transcript usage, (4) transcriptional event usage, and (5) splice-junction usage (Supplementary Figure 1). Quantification was performed using version v22.05.1 of the eQTL-Catalogue/rnaseq workflow implemented in Nextflow (Di Tommaso et al., 2017). Before quantification, we used Trim Galore v0.5.0 to remove sequencing adapters from the fastq files.

For gene expression quantification, we used HISAT2 v2.2.1 (Kim et al., 2019) to align reads to the GRCh38 reference genome (Homo_sapiens.GRCh38.dna.primary_assembly.fa file downloaded from Ensembl). We counted the number of reads overlapping the genes in the GENCODE V39 (Harrow et al., 2012) reference transcriptome annotations with featureCounts v1.6.4 (Liao et al., 2014). To quantify exon expression, we first created an exon annotation file (GFF) using GENCODE V39 reference transcriptome annotations and `dexseq_prepare_annotation.py` script from the DEXSeq (Anders et al., 2012) package. We then used the aligned RNA-seq BAM files from the gene expression quantification and featureCounts with flags '`-p -t exonic_part -s ${direction} -f -O`' to count the number of reads overlapping each exon.

We quantified transcript and event expression with Salmon v1.8.0 (Patro et al., 2017). For transcript quantification, we used the GENCODE V39 (GRCh38.p13) reference transcript sequences (fasta) file to build the Salmon index. For transcriptional event usage, we downloaded pre-computed txrevise (Alasoo et al., 2019; Vija and Alasoo, 2022) alternative promoter, splicing and alternative 3' end annotations corresponding to Ensembl version 105 from Zenodo (https://doi.org/10.5281/zenodo.6499127) in GFF format. These annotations had been augmented with additional experimentally derived promoter annotations from the FANTOM5 consortium (Abugessaisa et al., 2017; FANTOM Consortium and the RIKEN PMI and CLST et al., 2014). We then used gffread (Pertea and Pertea, 2020) to generate fasta sequences from the event annotations and built Salmon indices for each event set as we did for transcript usage. Finally, we quantified transcript and event expression using `salmon quant` with '`--seqBias --useVBOpt --gcBias --libType`' flags. All expression matrices were merged using csvtk v0.17.0. Our reference transcriptome annotations are available from Zenodo (https://doi.org/10.5281/zenodo.4715946).

For Leafcutter analysis, splice junctions of the aligned reads were extracted using the *junctions extract* command of the regtools v0.5.2 (Cotto et al., 2023) with options `'-s $strand -a 8 -m 50 -M 500000'`. Then, these splice-junctions were clustered using leafcutter_cluster_regtools.py script from LeafCutter v0.2.9 with options '`-m 50 -o leafcutter -l 500000 --checkchrom=True`'.

Normalisation. We normalised the gene and exon-level read counts using the conditional quantile normalisation (cqn) R package v1.30.0 (Hansen et al., 2012) with gene or exon GC nucleotide content as a covariate. We downloaded the gene GC content estimates from Ensembl biomaRt and calculated the exon-level GC content using bedtools v2.19.0 (Quinlan and Hall, 2010). We also excluded lowly expressed genes, where 95 per cent of the samples within a dataset had transcripts per million (TPM)-normalised expression less than 1. To calculate transcript and transcriptional event usage values, we obtained the TPM normalised transcript (event) expression estimates from Salmon. We then divided those transcript (event) expression estimates by the total expression of all transcripts (events) from the same gene (event group). Subsequently, we used the inverse normal transformation to standardise all five molecular quantification estimates. Normalisation scripts together with containerised software are publicly available at https://github.com/eQTL-Catalogue/qcnorm.

Association testing and statistical fine mapping

We performed association testing separately in each dataset and used a +/- 1 megabase *cis* window centred around the start of each gene. First, we excluded molecular traits with less than five genetic variants in their *cis* window, as these were likely to reside in regions with low genotyping coverage. We also excluded molecular traits with zero variance across all samples and calculated phenotype principal components using the prcomp R stats package (center = true, scale = true). We calculated genotype principal components using plink2 v1.90b3.35. We used the first six genotype and molecular trait principal components as covariates in QTL mapping. We calculated nominal eQTL summary statistics using the GTEx v6p version of the FastQTL (Ongen et al., 2016) software (https://github.com/francois-a/fastqtl) that also estimates standard errors of the effect sizes. We used the '`--window 1000000 --nominal 1`' flags to find all associations in 1 Mb *cis* window. For permutation analysis, we used QTLtools v1.3.1 (Delaneau et al., 2017) with '`--window 1000000 --permute 1000 --grp-best`' flags to calculate empirical p-values based on 1000 permutations. The '`--grp-best`' option ensured that the permutations were performed across all molecular traits within the same 'group' (e.g. multiple probes per gene in microarray data or multiple transcripts or exons per gene in the exon-level and transcript-level analysis) and the empirical p-value was calculated at the group level.

We performed QTL fine mapping using the Sum of Single Effects Model (SuSiE) (Wang et al., 2020) implemented in the susieR v0.11.92 R package. We converted the genotypes from VCF format to a tabix-indexed dosage matrix with bcftools v1.10.2. We imported the genotype dosage matrix into R using the Rsamtools v2.8.0 R package. We used the same normalised molecular trait matrix used for QTL mapping. We regressed out the first six phenotype and

genotype PCs separately from the phenotype and genotype matrices. We performed fine mapping with the following parameters: L = 10, estimate_residual_variance = TRUE, estimate_prior_variance = TRUE, scaled_prior_variance = 0.1, compute_univariate_zscore = TRUE, min_abs_corr = 0. The steps described above are implemented in the eQTL-Catalogue/qtlmap v22.04.01 Nextflow workflow available from GitHub.

Filtering of transcript-level summary statistics

We filtered transcript-level summary statistics using a connected components approach (Kolberg et al., 2020) to select the strongest signals per transcript-level group (gene for transcript and exon level, clusters for leafcutter). For each group, first, we filtered out the credible sets where maximum absolute z value is lower than 3 and size is bigger than 200 variants. Then, we found overlapping variants between credible sets, defining these credible sets as connected components. For each connected component we selected the molecular trait with the highest posterior inclusion probability (PIP) and kept only the summary statistics of these selected molecular traits. This approach enabled easier sharing of most significant signals per molecular trait group, decreasing the volume of shared data by 98%.

Colocalisation with vitamin D GWAS

We used coloc.susie (Wallace, 2021) to perform signal-level colocalisation between all RNA-seq-based datasets in the eQTL Catalogue and GWAS summary statistics for vitamin D levels in the UK Biobank. For all molecular QTLs, we used the log Bayes factors (LBFs) exported by our eQTL-Catalogue/qtlmap v22.04.01 workflow. For the vitamin D GWAS, we used published SuSiE fine mapping results from a previous study (Kanai et al., 2021) downloaded from Google Cloud (link). We performed colocalisation between all pairs of independent fine mapped signals (up to 10 per locus) and reported results where PP4 > 0.9. The colocalisation workflows is available from GitHub (https://github.com/ralf-tambets/coloc).

Generation of QTL coverage plots

We used the bamCoverage command from deepTools v3.2.0 (Ramírez et al., 2016) with bin-size option '`-bs 5`' to generate read-coverage (bigwig) files. We then used extractCoverageData and plotCoverageData commands of wiggleplotr R v1.13.1 package (Alasoo, 2017) to read specific regions of the bigwig files, scale all introns to the length of 50 nucleotides, and generate the plots as ggplot2 (Wickham, 2016) objects. Finally, we generated exon QTL effect-size plots with ggplot2 v3.3.6 and put all the plots together with the cowplot v1.1.1 R package (Wilke, 2019). We used *tabix.read.table* from seqminer v8.4 package (Zhan and Liu, 2015) to extract both genotype and QTL data from indexed files in the regions of interest. Coverage plot generation workflow is publicly available at https://github.com/kerimoff/leafcutter_plot.

Author contributions

N.K. and H.J.T performed quality control of individual-level data and executed the eQTL analysis workflows. N.K. generated the static QTL coverage plots for all molecular QTLs. R.T. modified the genotype imputation workflow to support imputation X chromosome genotypes. P.K. implemented the low-coverage WGS genotype imputation workflow. M.K., and J.C.U performed the fine-mapping analysis on vitamin D levels in the UK Biobank. R.T. implemented the fine mapping analysis for the eQTL Catalogue datasets and performed colocalisation between all molecular traits and vitamin D GWAS. A.V. updated the promoter annotations for txrevise. M.R., J.H., S.G., and D.T. prepared the Braineac2 dataset for eQTL analysis. H.J.T. performed quality control of newly added eQTL datasets. A.C., W.R. and S.K-H. used the eQTL Catalogue workflows to perform federated eQTL analysis on the Kim-Hellmuth_2017 dataset. J.D.H. implemented the eQTL Catalogue summary statistics REST API. I.K., U.R. and H. Peterson set up the eQTL Catalogue credible set browser. I.R. and K.A. performed literature review to prioritise causal genes at fine mapped GWAS loci. K.A, H.Parkinson, A.M and H.F. supervised the project. N.K. and K.A. wrote the manuscript with input from all authors.

Acknowledgements

The RNA-seq quantification and QTL analyses were performed at the High Performance Computing Center, University of Tartu. We thank O.E. Oopkaup, S. Kuusemets and the rest of the team of the High Performance Computing Center for their professional and timely technical support in enabling the analyses performed in this paper. We thank M. Weale for preparing the Braineac2 dataset for analysis. N.K., J.D.H., P.K. and H.J.T. were supported by a grant from Open Targets (grant no. OTAR2077). H. Parkinson, A.M. and J.H. were supported by the European Molecular Biology Laboratory. K.A., A.C., W.R. and N.K. also received funding from the European Union's Horizon 2020 research and innovation program (grant no. 825775). K.A., N.K, R.T., A.V., P.K. and I.R. were supported by the Estonian Research Council (grant nos. IUT34-4 and PSG415). K.A. and N.K. were also supported by the Estonian Centre of Excellence in ICT Research (EXCITE), funded by the European Regional Development Fund. I.K., U.R. and H. Peterson were supported by a Distributed Infrastructure for Life-Science Information ELIXIR, European Regional Development Fund project (2014-2020.4.01.16-0271). S.K.-H. was supported by the Emmy Noether Programme KI 2091/2-1 (459153572), SFB/TRR237-B29 (369799452) and SFB/TRR359-B06 (491676693) of the Deutsche Forschungsgemeinschaft (DFG). Funding information for individual studies included in the eQTL Catalogue is presented in Supplementary Note 2.

Competing interests

J.C.U. is an employee of Illumina. N.K. is an employee of Nightingale Health. M.W. is an employee of Genomics Plc. S.G. is an employee of Verge Genomics.

Data Availability

The molecular QTL summary statistics, fine mapping results (including SuSiE log Bayes factor) and QTL coverage plots are available from the eQTL Catalogue FTP server (see https://www.ebi.ac.uk/eqtl/Data_access/). The marginal eQTL summary statistics are also available via our REST API (https://wwwdev.ebi.ac.uk/eqtl/api/docs), which we have completely re-written for release 6. RNA-seq and genotype data from the CAP (phs000481.v3.p2), Peng_2018 (phs001586.v1.p1), PhLiPS (phs001341.v1.p1) and iPSCORE (phs000924.v4.p1) studies were downloaded from dbGaP; Steinberg_2020 (EGAD00001005215, EGAD00001003355, EGAD00010001746), Young_2019 (EGAD00001005736) and Bossini-Castillo_2019 (EGAD00001004830, EGAD00010001848) from EGA, and CommonMind (syn2759792) from Synapse. Raw genotype data for Gilchrist_2021 (EGAD00010000144, EGAD00010000520) was downloaded from EGA. Raw gene expression data from Gilchrist_2021 was downloaded from Zenodo (https://doi.org/10.5281/zenodo.6352656). Raw RNA-seq and genotype data from Braineac2 were not deposited.

Supplementary Note

Reference mapping bias is known to induce false positive associations in splicing and allele specific expression analysis (Kumasaka et al., 2016; Li et al., 2018; van de Geijn et al., 2015). A tool often used to correct for reference mapping bias is WASP (van de Geijn et al., 2015), which has also been included in the STAR (Dobin et al., 2013) RNA-seq short read aligner. Although the eQTL Catalogue uses HISAT2 (Kim et al., 2019) to perform RNA-seq read alignment, we did consider the option to switch to STAR to use WASP read filtering. However, after initial benchmarks we opted against it. First, we found that WASP was very conservative and filtered out a large proportion of reads form exonic regions. As a result, many well-known true positive splicing QTLs were no longer detected and the QTL read coverage plots became noisy due to the large number of filtered reads. Secondly, as implemented in STAR, WASP was only able to account for single nucleotide variants and did not consider short insertions or deletions that have even large potential to cause reference mapping bias. Finally, our transcript usage and txrevise quantification uses Salmon (Patro et al., 2017) to pseudoalign reads directly to the transcriptome and is thus not compatible with WASP. For example, two of the three suspected reference mapping bias cases (*DHCR7* and *NUDT9*) were detected in Salmon transcript usage analysis. Finally, switching to STAR+WASP would have significantly increased the runtime of our RNA-seq quantification workflow which already took over two months at the University of Tartu High Performance Computing Center. For these reasons we decided against directly correcting for reference mapping bias in the QTL mapping process. Instead, we opted to provide access to pre-generated QTL coverage plots that can be used to visually detect strong cases of reference mapping bias.

Supplementary Note 2

Funding statements for the new studies included in the eQTL Catalogue.

CommonMind. Bio-samples and/or data for this publication were obtained from NIMH Repository & Genomics Resource, a centralized national biorepository for genetic studies of psychiatric disorders. Data were generated as part of the CommonMind Consortium supported by funding from Takeda Pharmaceuticals Company Limited, F. Hoffman-La Roche Ltd and NIH grants R01MH085542, R01MH093725, P50MH066392, P50MH080405, R01MH097276, RO1-MH-075916, P50M096891, P50MH084053S1, R37MH057881, AG02219, AG05138, MH06692, R01MH110921, R01MH109677, R01MH109897, U01MH103392, and contract HHSN271201300031C through IRP NIMH. Brain tissue for the study was obtained from the following brain bank collections: the Mount Sinai NIH Brain and Tissue Repository, the University of Pennsylvania Alzheimer's Disease Core Center, the University of Pittsburgh NeuroBioBank and Brain and Tissue Repositories, and the NIMH Human Brain Collection Core. CMC Leadership: Panos Roussos, Joseph Buxbaum, Andrew Chess, Schahram Akbarian, Vahram Haroutunian (Icahn School of Medicine at Mount Sinai), Bernie Devlin, David Lewis (University of Pittsburgh), Raquel Gur, Chang-Gyu Hahn (University of Pennsylvania), Enrico Domenici (University of Trento), Mette A. Peters, Solveig Sieberts (Sage Bionetworks), Thomas Lehner, Stefano Marenco, Barbara K. Lipska (NIMH).

CAP. The dataset used for the analyses described in this manuscript was obtained from the Cholesterol and Pharmacogenetics (CAP) study through dbGAP (phs000481.v3.p2). Funding support for the generation of this dataset was provided by National Heart, Lung, Blood Institute (NHLBI) grant U01 HL69757. The manuscript was not prepared in collaboration with CAP investigators and does not necessarily reflect the opinions or views of CAP investigators or NHLBI.

Peng_2018. This work was supported by the National Institutes of Health [NIH-NIMH R01MH094609, NIH-NIEHS R01ES022223, NIH-NIEHS PO1ES022832, NIH-NIEHS R24ES028507, NIH-NIEHS R21ES028226, and NIH-NIEHS R01ES025145. A complete description of the cohort can be found in: Appleton AA, Murphy MA, Koestler DC, Lesseur C, Paquette AG, Padbury JF, Lester BM, and Marsit CJ. Prenatal Programming of Infant Neurobehavior in a Healthy Population. Paediatr Perinat Epidemiol 2016, 30(4): 367-75.

PhLiPS. This work was supported by grant 5U01HG006398.

iPSCORE. This work was supported in part by a California Institute for Regenerative Medicine (CIRM) grant GC1R-06673 and NIH grants EY021237, HG008118, HL107442, DK105541 and DK112155. iPSC RNA-seq was performed at the UCSD IGM Genomics Center with support from NIH grant P30 CA023100.

Bossini-Castillo_2019. This research was funded by the Wellcome Trust (grant number WT206194). L.B.-C. was supported by the MRC Skills Development Fellowship (MR/N014995/1).

Steinberg_2020. This work was funded by the Wellcome Trust (206194). M.J.C. was funded through a Medical Research Council Centre for Integrated Research into Musculoskeletal Ageing grant (148985). R.A.B. and the Human Research Tissue Bank are supported by the NIHR Cambridge Biomedical Research Centre. J.H.D.B. and G.R.W. are funded by a Wellcome Trust Strategic Award (101123), a Wellcome Trust Joint Investigator Award (110140 and 110141) and a European Commission Horizon 2020 Grant (666869, THYRAGE). A.W.M. receives funding from Versus Arthritis; Tissue Engineering and Regenerative Therapies Centre (21156).

Young_2019. R.F. was supported by funding from the UK Multiple Sclerosis Society (MS50), the Adelson Medical Research Foundation and a core support grant from the Wellcome Trust and MRC to the Wellcome Trust-Medical Research Council Cambridge Stem Cell Institute (203151/Z/16/Z). A.Y. is supported by a Wellcome Trust Clinicians PhD Fellowship (RRZD/029). All data for this study were generated under Open targets project OTAR039. N.K. and D.J.G. were funded by the Wellcome Trust grant WT206194.

Gilchrist_2021. C.K. was supported by Wellcome Trust Investigator Award [204969/Z/16/Z], NIHR Oxford Biomedical Research Centre and Chinese Academy of Medical Sciences (CAMS) Innovation 537 Fund for Medical Science (grant number: 2018-I2M-2-002), Wellcome Trust Grants 090532/Z/09/Z and 203141/Z/16/Z to core facilities Wellcome Centre for Human Genetics, Oxford Biomedical Research Computing (BMRC) facility, a joint development between the Wellcome Centre for Human Genetics and the Big Data Institute supported by Health Data Research UK and the NIHR Oxford Biomedical Research Centre. The study was funded by Wellcome Trust Intermediate Clinical Fellowship to B.P.F. (no. 201488/Z/16/Z). J.J.G. is funded by a National Institute for Health Research (NIHR) Clinical Lectureship.

Braineac2. Mina Ryten, David Zhang, and Karishma D'Sa were supported by the UK Medical Research Council (MRC) through the award of Tenure-track Clinician Scientist Fellowship to Mina Ryten (MR/N008324/1). Sebastian Guelfi was supported by Alzheimer's Research UK through the award of a PhD Fellowship (ARUK-PhD2014-16). Regina Reynolds was supported through the award of a Leonard Wolfson Doctoral Training Fellowship in Neurodegeneration. All RNA sequencing data performed as part of this study were generated by the commercial company AROS Applied Biotechnology A/S (Denmark).

Supplementary figures

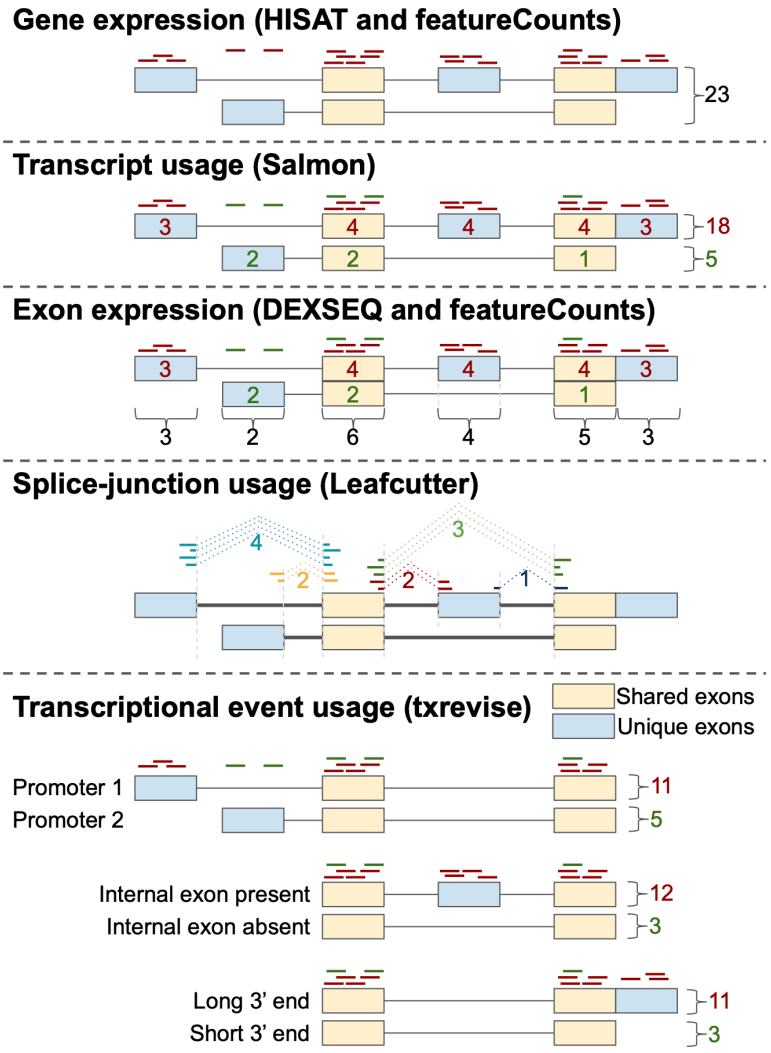

Supplementary Figure 1. Overview of the five molecular trait quantification methods used by the eQTL Catalogue. Gene expression was quantified by counting the total number of reads overlapping annotated exons of the gene. Transcript usage was estimated with Salmon. Exon expression was estimated by counting the number of reads overlapping each exon. Splice-junction usage was quantified with Leafcutter. Txrevise was used to estimate the expression levels of three types of transcriptional events (promoter usage, splicing and 3′ end usage).

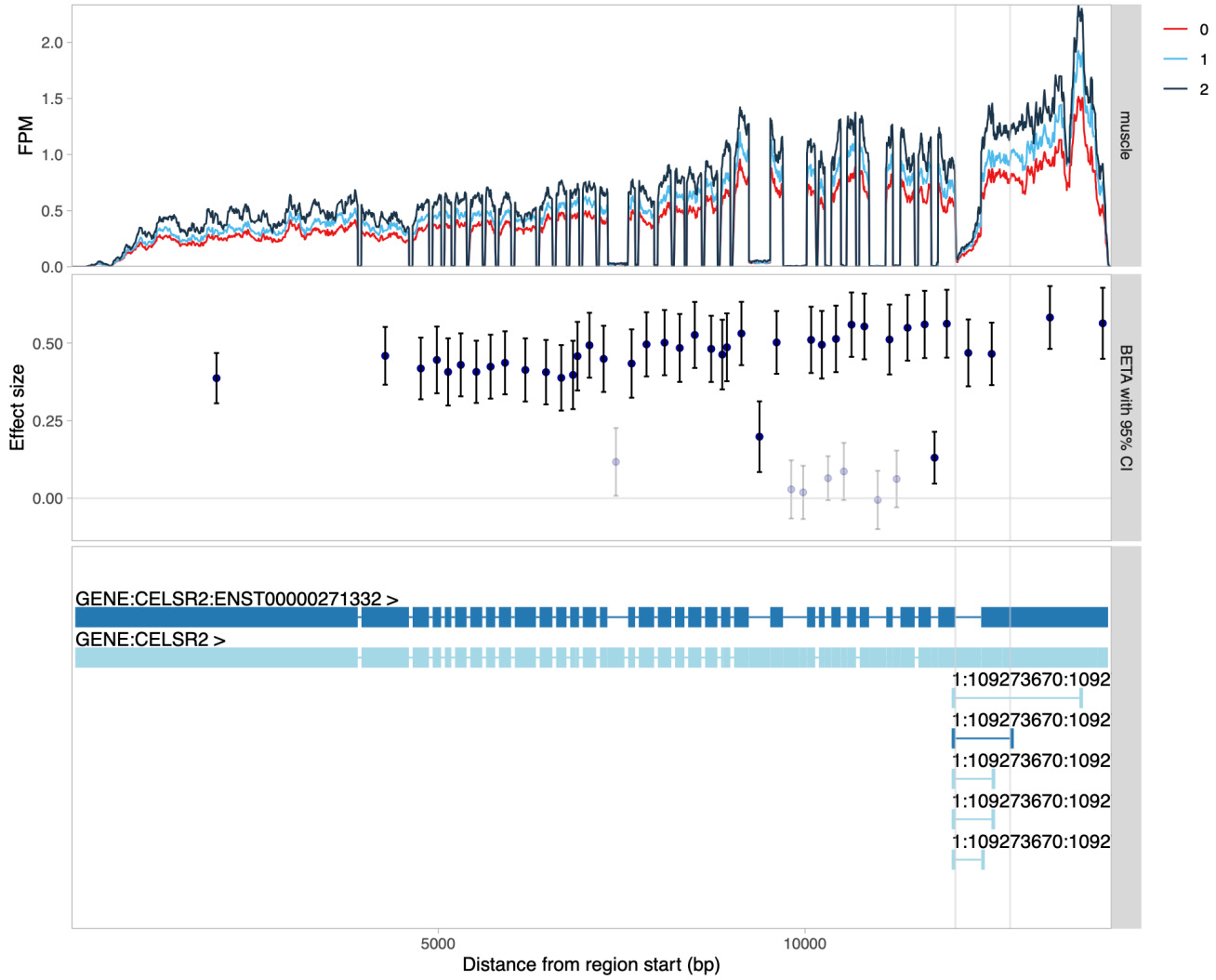

Supplementary Figure 2. QTL coverage plot for *CELSR2* gene stratified by the lead Leafcutter QTL variant (chr1_109274241_T_TC) in the GTEx muscle tissue. The observed association at junction reads in the 3' end of the gene is likely a consequence of the strong eQTL effect at this locus rather than the primary mechanism driving complex trait association.

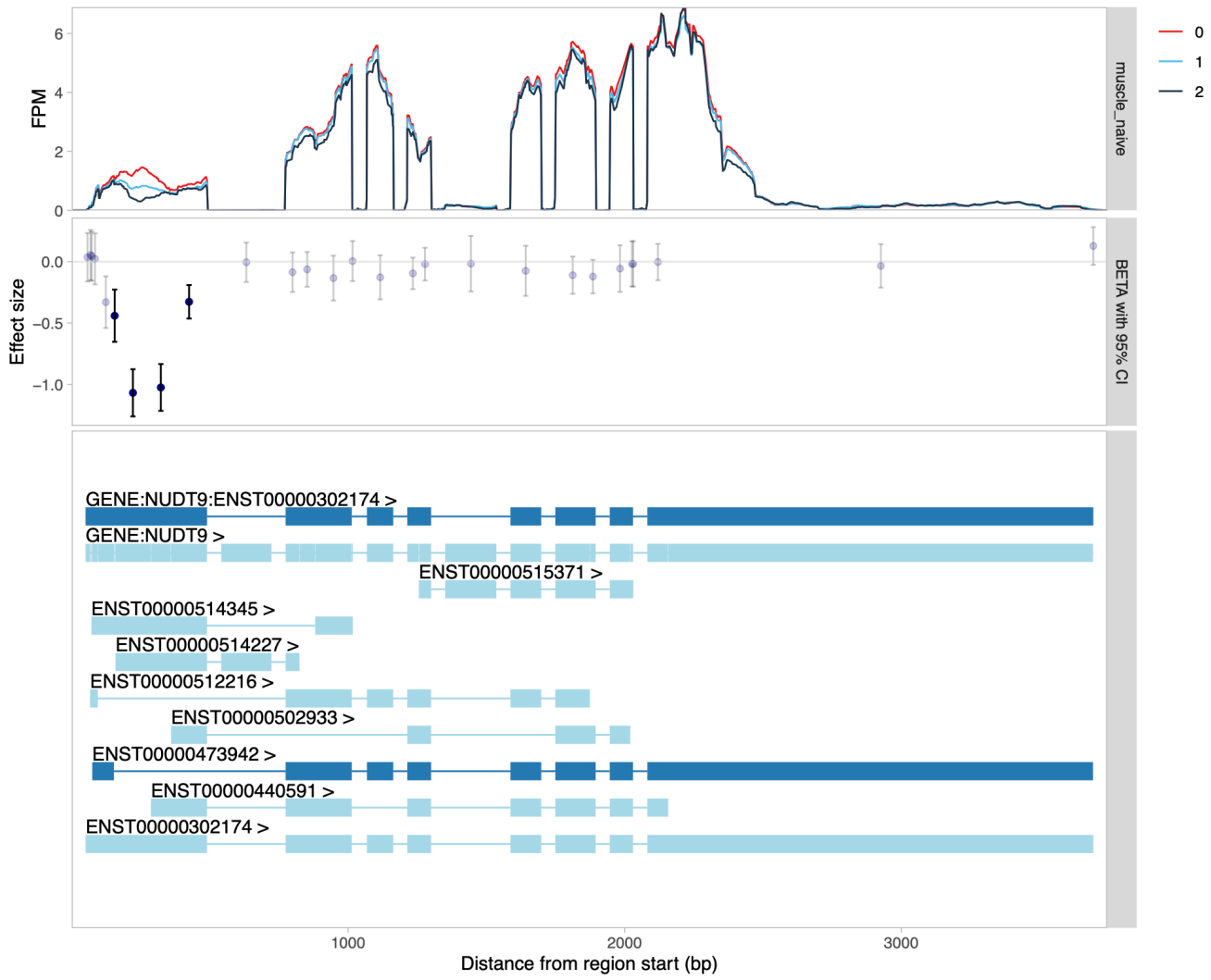

Supplementary Figure 3. QTL coverage plot for *NUDT9* stratified by the genotype of the lead transcript usage (tx) QTL variant (chr4_87380254_C_T) in the FUSION (Taylor et al., 2019) muscle tissue. The 'bulge' in read coverage observed at the 5' end of the gene suggests potential reference mapping bias.

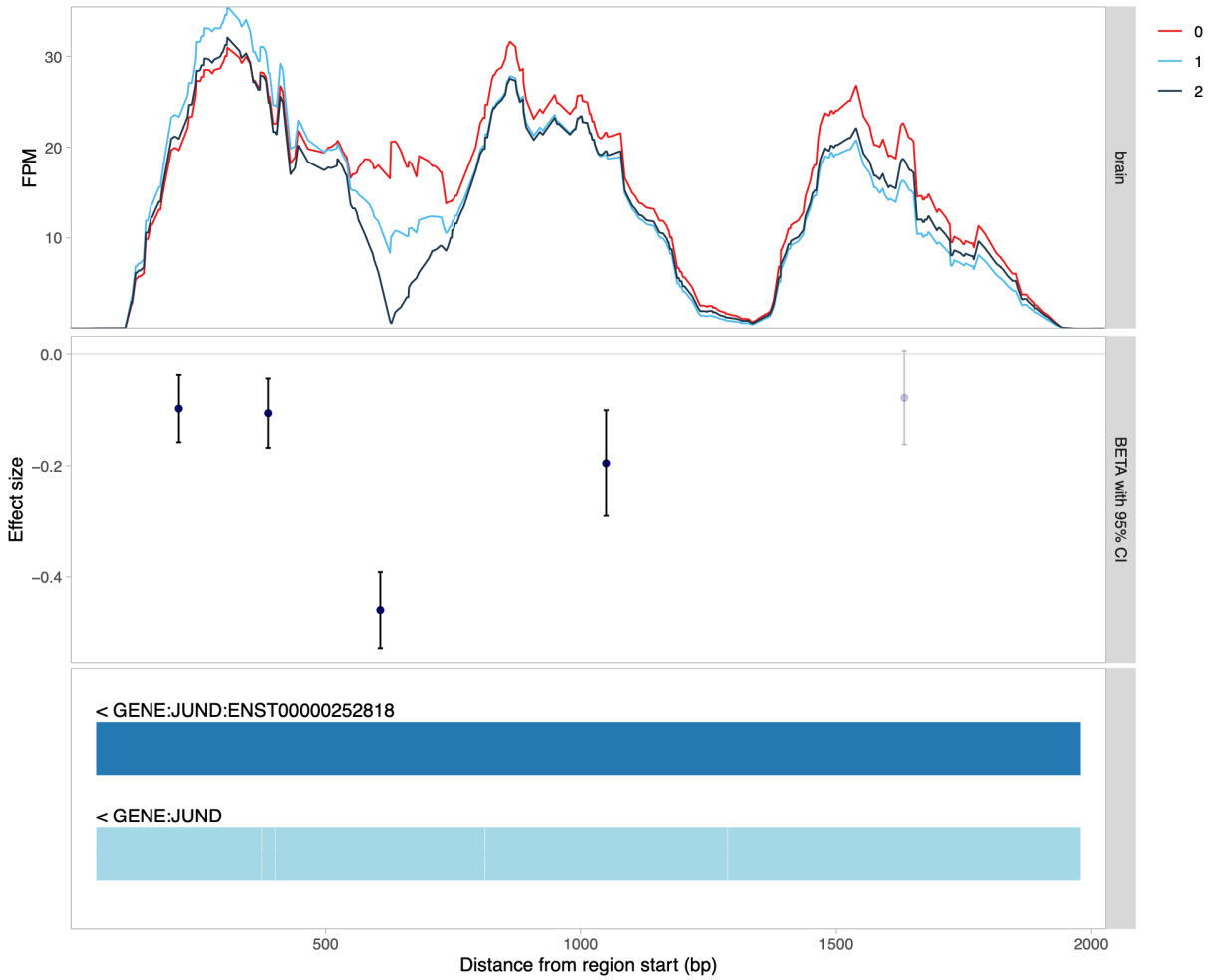

Supplementary Figure 4. QTL coverage plot for *JUND* stratified by the genotype of the lead gene expression (ge) QTL variant (chr19_18287220_A_C) in the BrainSeq (Jaffe et al., 2018) dataset. The drop in read coverage in the middle of the exon suggests potential reference mapping bias.

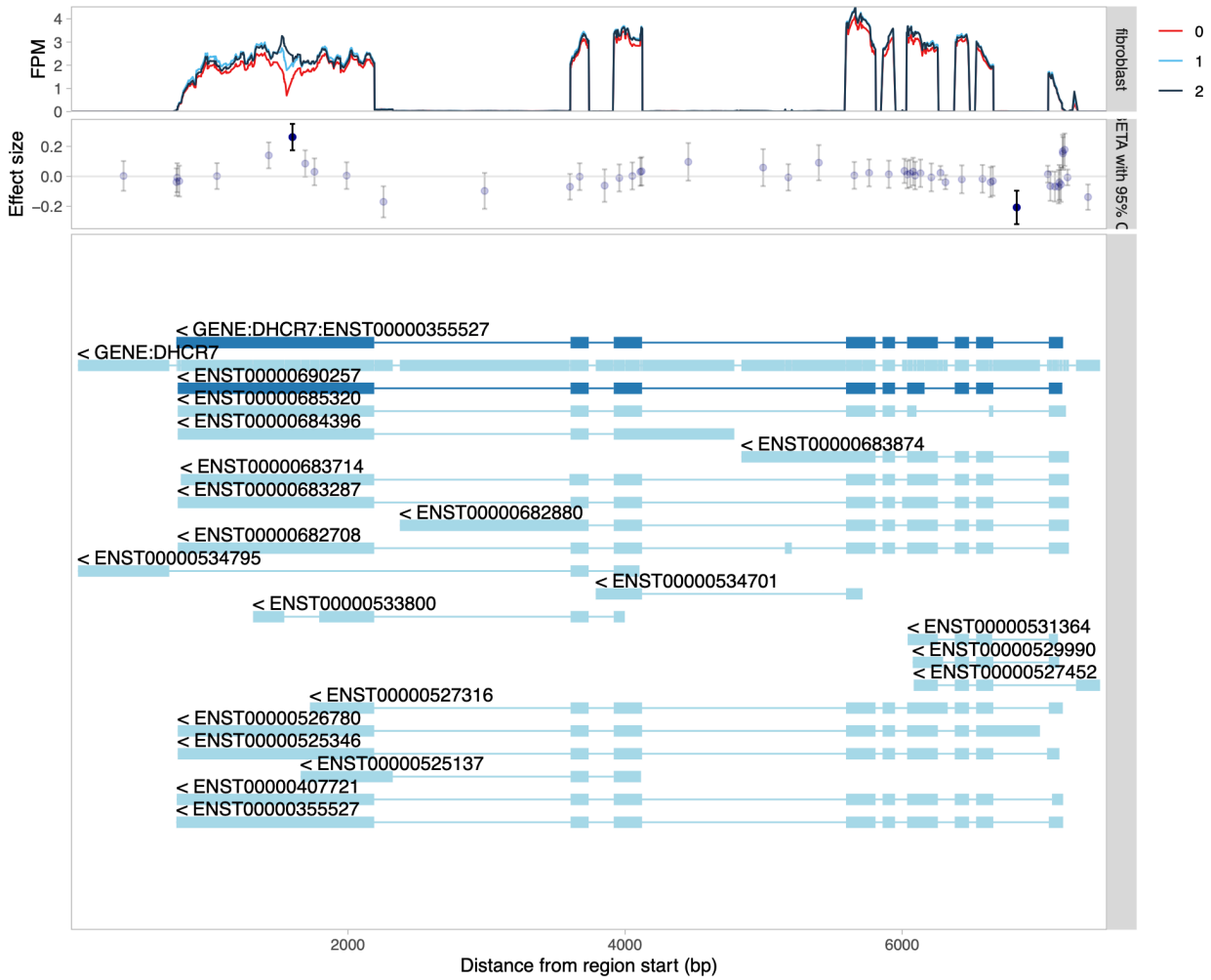

Supplementary Figure 5. QTL coverage plot for *DHCR7* stratified by the genotype of the lead transcript usage (tx) QTL variant (chr11_71458997_T_C) in the GTEx fibroblast dataset. The 'bulge' in read coverage observed at the middle of the last exon of the MANE Select transcript (ENST00000355527) suggests that the association is driven by reference mapping bias.

References

Abugessaisa I, Noguchi S, Hasegawa A, Harshbarger J, Kondo A, Lizio M, Severin J, Carninci P, Kawaji H, Kasukawa T. 2017. FANTOM5 CAGE profiles of human and mouse reprocessed for GRCh38 and GRCm38 genome assemblies. *Sci Data* **4**:170107.

Alasoo K. 2017. wiggleplotr: Make read coverage plots from BigWig files. Bioconductor. doi:10.18129/B9.bioc.wiggleplotr

Alasoo K, Rodrigues J, Danesh J, Freitag DF, Paul DS, Gaffney DJ. 2019. Genetic effects on promoter usage are highly context-specific and contribute to complex traits. *Elife* **8**. doi:10.7554/eLife.41673

Alasoo K, Rodrigues J, Mukhopadhyay S, Knights AJ, Mann AL, Kundu K, HIPSCI Consortium, Hale C, Dougan G, Gaffney DJ. 2018. Shared genetic effects on chromatin and gene expression indicate a role for enhancer priming in immune response. *Nat Genet* **50**:424–431.

Anders S, Reyes A, Huber W. 2012. Detecting differential usage of exons from RNA-seq data. *Genome Res* **22**:2008–2017.

Bossini-Castillo L, Glinos DA, Kunowska N, Golda G, Lamikanra AA, Spitzer M, Soskic B, Cano-Gamez E, Smyth DJ, Cattermole C, Alasoo K, Mann A, Kundu K, Lorenc A, Soranzo N, Dunham I, Roberts DJ, Trynka G. 2022. Immune disease variants modulate gene expression in regulatory CD4+ T cells. *Cell Genomics* **0**. doi:10.1016/j.xgen.2022.100117

Buil A, Brown AA, Lappalainen T, Viñuela A, Davies MN, Zheng H-F, Richards JB, Glass D, Small KS, Durbin R, Spector TD, Dermitzakis ET. 2015. Gene-gene and gene-environment interactions detected by transcriptome sequence analysis in twins. *Nat Genet* **47**:88–91.

Byrska-Bishop M, Evani US, Zhao X, Basile AO, Abel HJ, Regier AA, Corvelo A, Clarke WE, Musunuri R, Nagulapalli K, Fairley S, Runnels A, Winterkorn L, Lowy E, Eichler EE, Korbel JO, Lee C, Marschall T, Devine SE, Harvey WT, Zhou W, Mills RE, Rausch T, Kumar S, Alkan C, Hormozdiari F, Chong Z, Chen Y, Yang X, Lin J, Gerstein MB, Kai Y, Zhu Q, Yilmaz F, Xiao C, Flicek P, Germer S, Brand H, Hall IM, Talkowski ME, Narzisi G, Zody MC. 2022. High-coverage whole-genome sequencing of the expanded 1000 Genomes Project cohort including 602 trios. *Cell* **185**:3426–3440.e19.

Cheng JB, Motola DL, Mangelsdorf DJ, Russell DW. 2003. De-orphanization of cytochrome P450 2R1: a microsomal vitamin D 25-hydroxilase. *J Biol Chem* **278**:38084–38093.

Chen L, Ge B, Casale FP, Vasquez L, Kwan T, Garrido-Martín D, Watt S, Yan Y, Kundu K, Ecker S, Datta A, Richardson D, Burden F, Mead D, Mann AL, Fernandez JM, Rowlston S, Wilder SP, Farrow S, Shao X, Lambourne JJ, Redensek A, Albers CA, Amstislavskiy V, Ashford S, Berentsen K, Bomba L, Bourque G, Bujold D, Busche S, Caron M, Chen S-H, Cheung W, Delaneau O, Dermitzakis ET, Elding H, Colgiu I, Bagger FO, Flicek P, Habibi E, Iotchkova V, Janssen-Megens E, Kim B, Lehrach H, Lowy E, Mandoli A, Matarese F, Maurano MT, Morris JA, Pancaldi V, Pourfarzad F, Rehnstrom K, Rendon A, Risch T, Sharifi N, Simon M-M, Sultan M, Valencia A, Walter K, Wang S-Y, Frontini M, Antonarakis SE, Clarke L, Yaspo M-L, Beck S, Guigo R, Rico D, Martens JHA, Ouwehand WH, Kuijpers TW, Paul DS, Stunnenberg HG, Stegle O, Downes K, Pastinen T, Soranzo N. 2016. Genetic Drivers of Epigenetic and Transcriptional Variation in Human Immune Cells. *Cell* **167**:1398–1414.e24.

Cotto KC, Feng Y-Y, Ramu A, Richters M, Freshour SL, Skidmore ZL, Xia H, McMichael JF, Kunisaki J, Campbell KM, Chen TH-P, Rozycki EB, Adkins D, Devarakonda S, Sankararaman S, Lin Y, Chapman WC, Maher CA, Arora V, Dunn GP, Uppaluri R, Govindan R, Griffith OL, Griffith M. 2023. Integrated analysis of genomic and transcriptomic data for the discovery of splice-associated variants in cancer. *Nat Commun* **14**:1–18.

Das S, Forer L, Schönherr S, Sidore C, Locke AE, Kwong A, Vrieze SI, Chew EY, Levy S,

McGue M, Schlessinger D, Stambolian D, Loh P-R, Iacono WG, Swaroop A, Scott LJ, Cucca F, Kronenberg F, Boehnke M, Abecasis GR, Fuchsberger C. 2016. Next-generation genotype imputation service and methods. *Nat Genet* **48**:1284–1287.

DeBoever C, Li H, Jakubosky D, Benaglio P, Reyna J, Olson KM, Huang H, Biggs W, Sandoval E, D'Antonio M, Jepsen K, Matsui H, Arias A, Ren B, Nariai N, Smith EN, D'Antonio-Chronowska A, Farley EK, Frazer KA. 2017. Large-Scale Profiling Reveals the Influence of Genetic Variation on Gene Expression in Human Induced Pluripotent Stem Cells. *Cell Stem Cell* **20**:533–546.e7.

Deelen P, Bonder MJ, van der Velde KJ, Westra H-J, Winder E, Hendriksen D, Franke L, Swertz MA. 2014. Genotype harmonizer: automatic strand alignment and format conversion for genotype data integration. *BMC Res Notes* **7**:901.

Degner JF, Pai AA, Pique-Regi R, Veyrieras J-B, Gaffney DJ, Pickrell JK, De Leon S, Michelini K, Lewellen N, Crawford GE, Stephens M, Gilad Y, Pritchard JK. 2012. DNase I sensitivity QTLs are a major determinant of human expression variation. *Nature* **482**:390–394.

Delaneau O, Ongen H, Brown AA, Fort A, Panousis NI, Dermitzakis ET. 2017. A complete tool set for molecular QTL discovery and analysis. *Nat Commun* **8**:15452.

Di Tommaso P, Chatzou M, Floden EW, Barja PP, Palumbo E, Notredame C. 2017. Nextflow enables reproducible computational workflows. *Nat Biotechnol* **35**:316–319.

Dobin A, Davis CA, Schlesinger F, Drenkow J, Zaleski C, Jha S, Batut P, Chaisson M, Gingeras TR. 2013. STAR: ultrafast universal RNA-seq aligner. *Bioinformatics* **29**:15–21.

Engreitz JM, Haines JE, Perez EM, Munson G, Chen J, Kane M, McDonel PE, Guttman M, Lander ES. 2016. Local regulation of gene expression by lncRNA promoters, transcription and splicing. *Nature*. doi:10.1038/nature20149

Fairfax BP, Humburg P, Makino S, Naranbhai V, Wong D, Lau E, Jostins L, Plant K, Andrews R, McGee C, Knight JC. 2014. Innate immune activity conditions the effect of regulatory variants upon monocyte gene expression. *Science* **343**:1246949.

Fairfax BP, Makino S, Radhakrishnan J, Plant K, Leslie S, Dilthey A, Ellis P, Langford C, Vannberg FO, Knight JC. 2012. Genetics of gene expression in primary immune cells identifies cell type-specific master regulators and roles of HLA alleles. *Nat Genet* **44**:502–510.

FANTOM Consortium and the RIKEN PMI and CLST, Forrest ARR, Kawaji H, Rehli M, Baillie JK, de Hoon MJL, Haberle V, Lassmann T, Kulakovskiy IV, Lizio M, Itoh M, Andersson R, Mungall CJ, Meehan TF, Schmeier S, Bertin N, Jørgensen M, Dimont E, Arner E, Schmidl C, Schaefer U, Medvedeva YA, Plessy C, Vitezic M, Severin J, Semple CA, Ishizu Y, Young RS, Francescatto M, Alam I, Albanese D, Altschuler GM, Arakawa T, Archer JAC, Arner P, Babina M, Rennie S, Balwierz PJ, Beckhouse AG, Pradhan-Bhatt S, Blake JA, Blumenthal A, Bodega B, Bonetti A, Briggs J, Brombacher F, Burroughs AM, Califano A, Cannistraci CV, Carbajo D, Chen Y, Chierici M, Ciani Y, Clevers HC, Dalla E, Davis CA, Detmar M, Diehl AD, Dohi T, Drabløs F, Edge ASB, Edinger M, Ekwall K, Endoh M, Enomoto H, Fagiolini M, Fairbairn L, Fang H, Farach-Carson MC, Faulkner GJ, Favorov AV, Fisher ME, Frith MC, Fujita R, Fukuda S, Furlanello C, Furino M, Furusawa J-I, Geijtenbeek TB, Gibson AP, Gingeras T, Goldowitz D, Gough J, Guhl S, Guler R, Gustincich S, Ha TJ, Hamaguchi M, Hara M, Harbers M, Harshbarger J, Hasegawa A, Hasegawa Y, Hashimoto T, Herlyn M, Hitchens KJ, Ho Sui SJ, Hofmann OM, Hoof I, Hori F, Huminiecki L, Iida K, Ikawa T, Jankovic BR, Jia H, Joshi A, Jurman G, Kaczkowski B, Kai C, Kaida K, Kaiho A, Kajiyama K, Kanamori-Katayama M, Kasianov AS, Kasukawa T, Katayama S, Kato S, Kawaguchi S, Kawamoto H, Kawamura YI, Kawashima T, Kempfle JS, Kenna TJ, Kere J, Khachigian LM, Kitamura T, Klinken SP, Knox AJ, Kojima M, Kojima S, Kondo N, Koseki H, Koyasu S, Krampitz S, Kubosaki A, Kwon AT, Laros JFJ, Lee W, Lennartsson A, Li K, Lilje B, Lipovich L, Mackay-Sim A, Manabe R-I, Mar JC, Marchand B, Mathelier A, Mejhert N, Meynert A, Mizuno Y, de Lima Morais DA, Morikawa H, Morimoto

M, Moro K, Motakis E, Motohashi H, Mummery CL, Murata M, Nagao-Sato S, Nakachi Y, Nakahara F, Nakamura T, Nakamura Y, Nakazato K, van Nimwegen E, Ninomiya N, Nishiyori H, Noma S, Noma S, Noazaki T, Ogishima S, Ohkura N, Ohimiya H, Ohno H, Ohshima M, Okada-Hatakeyama M, Okazaki Y, Orlando V, Ovchinnikov DA, Pain A, Passier R, Patrikakis M, Persson H, Piazza S, Prendergast JGD, Rackham OJL, Ramilowski JA, Rashid M, Ravasi T, Rizzu P, Roncador M, Roy S, Rye MB, Saijyo E, Sajantila A, Saka A, Sakaguchi S, Sakai M, Sato H, Savvi S, Saxena A, Schneider C, Schultes EA, Schulze-Tanzil GG, Schwegmann A, Sengstag T, Sheng G, Shimoji H, Shimoni Y, Shin JW, Simon C, Sugiyama D, Sugiyama T, Suzuki M, Suzuki N, Swoboda RK, 't Hoen PAC, Tagami M, Takahashi N, Takai J, Tanaka H, Tatsukawa H, Tatum Z, Thompson M, Toyodo H, Toyoda T, Valen E, van de Wetering M, van den Berg LM, Verado R, Vijayan D, Vorontsov IE, Wasserman WW, Watanabe S, Wells CA, Winteringham LN, Wolvetang E, Wood EJ, Yamaguchi Y, Yamamoto M, Yoneda M, Yonekura Y, Yoshida S, Zabierowski SE, Zhang PG, Zhao X, Zucchelli S, Summers KM, Suzuki H, Daub CO, Kawai J, Heutink P, Hide W, Freeman TC, Lenhard B, Bajic VB, Taylor MS, Makeev VJ, Sandelin A, Hume DA, Carninci P, Hayashizaki Y. 2014. A promoter-level mammalian expression atlas. *Nature* **507**:462–470.

Fulco CP, Nasser J, Jones TR, Munson G, Bergman DT, Subramanian V, Grossman SR, Anyoha R, Doughty BR, Patwardhan TA, Nguyen TH, Kane M, Perez EM, Durand NC, Lareau CA, Stamenova EK, Aiden EL, Lander ES, Engreitz JM. 2019. Activity-by-contact model of enhancer-promoter regulation from thousands of CRISPR perturbations. *Nat Genet* **51**:1664–1669.

Garieri M, Delaneau O, Santoni F, Fish RJ, Mull D, Carninci P, Dermitzakis ET, Antonarakis SE, Fort A. 2017. The effect of genetic variation on promoter usage and enhancer activity. *Nat Commun* **8**:1358.

Gilchrist JJ, Makino S, Naranbhai V, Sharma PK, Koturan S, Tong O, Taylor CA, Watson RA, de Los Aires AV, Cooper R, Lau E, Danielli S, Hameiri-Bowen D, Lee W, Ng E, Whalley J, Knight JC, Fairfax BP. 2022. Natural Killer cells demonstrate distinct eQTL and transcriptome-wide disease associations, highlighting their role in autoimmunity. *Nat Commun* **13**:4073.

Guelfi S, D'Sa K, Botía JA, Vandrovcova J, Reynolds RH, Zhang D, Trabzuni D, Collado-Torres L, Thomason A, Quijada Leyton P, Gagliano Taliun SA, Nalls MA, International Parkinson's Disease Genomics Consortium (IPDGC), UK Brain Expression Consortium (UKBEC), Small KS, Smith C, Ramasamy A, Hardy J, Weale ME, Ryten M. 2020. Regulatory sites for splicing in human basal ganglia are enriched for disease-relevant information. *Nat Commun* **11**:1041.

Gutierrez-Arcelus M, Lappalainen T, Montgomery SB, Buil A, Ongen H, Yurovsky A, Bryois J, Giger T, Romano L, Planchon A, Falconnet E, Bielser D, Gagnebin M, Padioleau I, Borel C, Letourneau A, Makrythanasis P, Guipponi M, Gehrig C, Antonarakis SE, Dermitzakis ET. 2013. Passive and active DNA methylation and the interplay with genetic variation in gene regulation. *Elife* **2**:e00523.

Hansen KD, Irizarry RA, Wu Z. 2012. Removing technical variability in RNA-seq data using conditional quantile normalization. *Biostatistics* **13**:204–216.

Harrow J, Frankish A, Gonzalez JM, Tapanari E, Diekhans M, Kokocinski F, Aken BL, Barrell D, Zadissa A, Searle S, Barnes I, Bignell A, Boychenko V, Hunt T, Kay M, Mukherjee G, Rajan J, Despacio-Reyes G, Saunders G, Steward C, Harte R, Lin M, Howald C, Tanzer A, Derrien T, Chrast J, Walters N, Balasubramanian S, Pei B, Tress M, Rodriguez JM, Ezkurdia I, van Baren J, Brent M, Haussler D, Kellis M, Valencia A, Reymond A, Gerstein M, Guigó R, Hubbard TJ. 2012. GENCODE: the reference human genome annotation for The ENCODE Project. *Genome Res* **22**:1760–1774.

Hoffman GE, Bendl J, Voloudakis G, Montgomery KS, Sloofman L, Wang Y-C, Shah HR,

Hauberg ME, Johnson JS, Girdhar K, Song L, Fullard JF, Kramer R, Hahn C-G, Gur R, Marenco S, Lipska BK, Lewis DA, Haroutunian V, Hemby S, Sullivan P, Akbarian S, Chess A, Buxbaum JD, Crawford GE, Domenici E, Devlin B, Sieberts SK, Peters MA, Roussos P. 2019. CommonMind Consortium provides transcriptomic and epigenomic data for Schizophrenia and Bipolar Disorder. *Sci Data* **6**:180.

Hyppönen E, Vimaleswaran KS, Zhou A. 2022. Genetic Determinants of 25-Hydroxyvitamin D Concentrations and Their Relevance to Public Health. *Nutrients* **14**. doi:10.3390/nu14204408

Jaffe AE, Straub RE, Shin JH, Tao R, Gao Y, Collado-Torres L, Kam-Thong T, Xi HS, Quan J, Chen Q, Colantuoni C, Ulrich WS, Maher BJ, Deep-Soboslay A, BrainSeq Consortium, Cross AJ, Brandon NJ, Leek JT, Hyde TM, Kleinman JE, Weinberger DR. 2018. Developmental and genetic regulation of the human cortex transcriptome illuminate schizophrenia pathogenesis. *Nat Neurosci* **21**:1117–1125.

Jaganathan K, Panagiotopoulou SK, McRae JF, Darbandi SF, Knowles D, Li YI, Kosmicki JA, Arbelaez J, Cui W, Schwartz GB, Chow ED, Kanterakis E, Gao H, Kia A, Batzoglou S, Sanders SJ, Farh KK-H. 2019. Predicting Splicing from Primary Sequence with Deep Learning. *Cell* **0**. doi:10.1016/j.cell.2018.12.015

Kanai M, Ulirsch JC, Karjalainen J, Kurki M, Karczewski KJ, Fauman E, Wang QS, Jacobs H, Aguet F, Ardlie KG, Kerimov N, Alasoo K, Benner C, Ishigaki K, Sakaue S, Reilly S, Kamatani Y, Matsuda K, Palotie A, Neale BM, Tewhey R, Sabeti PC, Okada Y, Daly MJ, Finucane HK, The BioBank Japan Project, FinnGen. 2021. Insights from complex trait fine-mapping across diverse populations. *bioRxiv*. doi:10.1101/2021.09.03.21262975

Kasela S, Daniloski Z, Bollepalli S, Jordan TX, tenOever BR, Sanjana NE, Lappalainen T. 2021. Integrative approach identifies SLC6A20 and CXCR6 as putative causal genes for the COVID-19 GWAS signal in the 3p21.31 locus. *Genome Biol* **22**:1–10.

Kasela S, Kisand K, Tserel L, Kaleviste E, Remm A, Fischer K, Esko T, Westra H-J, Fairfax BP, Makino S, Knight JC, Franke L, Metspalu A, Peterson P, Milani L. 2017. Pathogenic implications for autoimmune mechanisms derived by comparative eQTL analysis of CD4+ versus CD8+ T cells. *PLoS Genet* **13**:e1006643.

Kerimov N, Hayhurst JD, Peikova K, Manning JR, Walter P, Kolberg L, Samoviča M, Sakthivel MP, Kuzmin I, Trevanion SJ, Burdett T, Jupp S, Parkinson H, Papatheodorou I, Yates AD, Zerbino DR, Alasoo K. 2021. A compendium of uniformly processed human gene expression and splicing quantitative trait loci. *Nat Genet* **53**:1290–1299.

Kilpinen H, Goncalves A, Leha A, Afzal V, Alasoo K, Ashford S, Bala S, Bensaddek D, Casale FP, Culley OJ, Danecek P, Faulconbridge A, Harrison PW, Kathuria A, McCarthy D, McCarthy SA, Meleckyte R, Memari Y, Moens N, Soares F, Mann A, Streeter I, Agu CA, Alderton A, Nelson R, Harper S, Patel M, White A, Patel SR, Clarke L, Halai R, Kirton CM, Kolb-Kokocinski A, Beales P, Birney E, Danovi D, Lamond AI, Ouwehand WH, Vallier L, Watt FM, Durbin R, Stegle O, Gaffney DJ. 2017. Common genetic variation drives molecular heterogeneity in human iPSCs. *Nature* **546**:370–375.

Kim D, Paggi JM, Park C, Bennett C, Salzberg SL. 2019. Graph-based genome alignment and genotyping with HISAT2 and HISAT-genotype. *Nat Biotechnol* **37**:907–915.

Kim-Hellmuth S, Bechheim M, Pütz B, Mohammadi P, Nédélec Y, Giangreco N, Becker J, Kaiser V, Fricker N, Beier E, Boor P, Castel SE, Nöthen MM, Barreiro LB, Pickrell JK, Müller-Myhsok B, Lappalainen T, Schumacher J, Hornung V. 2017. Genetic regulatory effects modified by immune activation contribute to autoimmune disease associations. *Nat Commun* **8**:266.

Kolberg L, Kerimov N, Peterson H, Alasoo K. 2020. Co-expression analysis reveals interpretable gene modules controlled by trans-acting genetic variants. *Elife* **9**. doi:10.7554/eLife.58705

Kumasaka N, Knights AJ, Gaffney DJ. 2018. High-resolution genetic mapping of putative causal

interactions between regions of open chromatin. *Nat Genet*. doi:10.1038/s41588-018-0278-6

Kumasaka N, Knights AJ, Gaffney DJ. 2016. Fine-mapping cellular QTLs with RASQUAL and ATAC-seq. *Nat Genet* **48**:206–213.

Kundu K, Mann AL, Tardaguila M, Watt S, Ponstingl H, Vasquez L, Morrell NW, Stegle O, Pastinen T, Sawcer SJ, Anderson CA, Walter K, Soranzo N. 2020. Genetic associations at regulatory phenotypes improve fine-mapping of causal variants for twelve immune-mediated diseases. *bioRxiv*. doi:10.1101/2020.01.15.907436

Lappalainen T, Sammeth M, Friedländer MR, 't Hoen PAC, Monlong J, Rivas MA, Gonzàlez-Porta M, Kurbatova N, Griebel T, Ferreira PG, Barann M, Wieland T, Greger L, van Iterson M, Almlöf J, Ribeca P, Pulyakhina I, Esser D, Giger T, Tikhonov A, Sultan M, Bertier G, MacArthur DG, Lek M, Lizano E, Buermans HPJ, Padioleau I, Schwarzmayr T, Karlberg O, Ongen H, Kilpinen H, Beltran S, Gut M, Kahlem K, Amstislavskiy V, Stegle O, Pirinen M, Montgomery SB, Donnelly P, McCarthy MI, Flicek P, Strom TM, Geuvadis Consortium, Lehrach H, Schreiber S, Sudbrak R, Carracedo A, Antonarakis SE, Häsler R, Syvänen A-C, van Ommen G-J, Brazma A, Meitinger T, Rosenstiel P, Guigó R, Gut IG, Estivill X, Dermitzakis ET. 2013. Transcriptome and genome sequencing uncovers functional variation in humans. *Nature* **501**:506–511.

Lepik K, Annilo T, Kukuškina V, Kisand K, Kutalik Z, Peterson P, Peterson H, eQTLGen Consortium. 2017. C-reactive protein upregulates the whole blood expression of CD59 - an integrative analysis. *PLoS Comput Biol* **13**:e1005766.

Liao Y, Smyth GK, Shi W. 2014. featureCounts: an efficient general purpose program for assigning sequence reads to genomic features. *Bioinformatics* **30**:923–930.

Li H. 2013. Aligning sequence reads, clone sequences and assembly contigs with BWA-MEM. *arXiv [q-bioGN]*.

Li YI, Knowles DA, Humphrey J, Barbeira AN, Dickinson SP, Im HK, Pritchard JK. 2018. Annotation-free quantification of RNA splicing using LeafCutter. *Nat Genet* **50**:151–158.

Li YI, van de Geijn B, Raj A, Knowles DA, Petti AA, Golan D, Gilad Y, Pritchard JK. 2016. RNA splicing is a primary link between genetic variation and disease. *Science* **352**:600–604.

Loh P-R, Danecek P, Palamara PF, Fuchsberger C, A Reshef Y, K Finucane H, Schoenherr S, Forer L, McCarthy S, Abecasis GR, Durbin R, L Price A. 2016. Reference-based phasing using the Haplotype Reference Consortium panel. *Nat Genet* **48**:1443–1448.

Manousaki D, Mitchell R, Dudding T, Haworth S, Harroud A, Forgetta V, Shah RL, Luan J 'an, Langenberg C, Timpson NJ, Richards JB. 2020. Genome-wide Association Study for Vitamin D Levels Reveals 69 Independent Loci. *Am J Hum Genet*. doi:10.1016/j.ajhg.2020.01.017

Maurano MT, Humbert R, Rynes E, Thurman RE, Haugen E, Wang H, Reynolds AP, Sandstrom R, Qu H, Brody J, Shafer A, Neri F, Lee K, Kutyavin T, Stehling-Sun S, Johnson AK, Canfield TK, Giste E, Diegel M, Bates D, Hansen RS, Neph S, Sabo PJ, Heimfeld S, Raubitschek A, Ziegler S, Cotsapas C, Sotoodehnia N, Glass I, Sunyaev SR, Kaul R, Stamatoyannopoulos JA. 2012. Systematic localization of common disease-associated variation in regulatory DNA. *Science* **337**:1190–1195.

Mittleman BE, Pott S, Warland S, Zeng T, Mu Z, Kaur M, Gilad Y, Li Y. 2020. Alternative polyadenylation mediates genetic regulation of gene expression. *Elife* **9**. doi:10.7554/eLife.57492

Momozawa Y, Dmitrieva J, Théâtre E, Deffontaine V, Rahmouni S, Charloteaux B, Crins F, Docampo E, Elansary M, Gori A-S, Lecut C, Mariman R, Mni M, Oury C, Altukhov I, Alexeev D, Aulchenko Y, Amininejad L, Bouma G, Hoentjen F, Löwenberg M, Oldenburg B, Pierik MJ, Vander Meulen-de Jong AE, Janneke van der Woude C, Visschedijk MC, International IBD Genetics Consortium, Lathrop M, Hugot J-P, Weersma RK, De Vos M, Franchimont D, Vermeire S, Kubo M, Louis E, Georges M. 2018. IBD risk loci are enriched

in multigenic regulatory modules encompassing putative causative genes. *Nat Commun* **9**:2427.

Morales J, Pujar S, Loveland JE, Astashyn A, Bennett R, Berry A, Cox E, Davidson C, Ermolaeva O, Farrell CM, Fatima R, Gil L, Goldfarb T, Gonzalez JM, Haddad D, Hardy M, Hunt T, Jackson J, Joardar VS, Kay M, Kodali VK, McGarvey KM, McMahon A, Mudge JM, Murphy DN, Murphy MR, Rajput B, Rangwala SH, Riddick LD, Thibaud-Nissen F, Threadgold G, Vatsan AR, Wallin C, Webb D, Flicek P, Birney E, Pruitt KD, Frankish A, Cunningham F, Murphy TD. 2022. A joint NCBI and EMBL-EBI transcript set for clinical genomics and research. *Nature* **604**:310–315.

Mountjoy E, Schmidt EM, Carmona M, Schwartzentruber J, Peat G, Miranda A, Fumis L, Hayhurst J, Buniello A, Karim MA, Wright D, Hercules A, Papa E, Fauman EB, Barrett JC, Todd JA, Ochoa D, Dunham I, Ghoussaini M. 2021. An open approach to systematically prioritize causal variants and genes at all published human GWAS trait-associated loci. *Nat Genet* 1–7.

Naranbhai V, Fairfax BP, Makino S, Humburg P, Wong D, Ng E, Hill AVS, Knight JC. 2015. Genomic modulators of gene expression in human neutrophils. *Nat Commun* **6**:7545.

Nasser J, Bergman DT, Fulco CP, Guckelberger P, Doughty BR, Patwardhan TA, Jones TR, Nguyen TH, Ulirsch JC, Lekschas F, Mualim K, Natri HM, Weeks EM, Munson G, Kane M, Kang HY, Cui A, Ray JP, Eisenhaure TM, Collins RL, Dey K, Pfister H, Price AL, Epstein CB, Kundaje A, Xavier RJ, Daly MJ, Huang H, Finucane HK, Hacohen N, Lander ES, Engreitz JM. 2021. Genome-wide enhancer maps link risk variants to disease genes. *Nature* 1–6.

Nédélec Y, Sanz J, Baharian G, Szpiech ZA, Pacis A, Dumaine A, Grenier J-C, Freiman A, Sams AJ, Hebert S, Pagé Sabourin A, Luca F, Blekhman R, Hernandez RD, Pique-Regi R, Tung J, Yotova V, Barreiro LB. 2016. Genetic Ancestry and Natural Selection Drive Population Differences in Immune Responses to Pathogens. *Cell* **167**:657–669.e21.

Ng B, White CC, Klein H-U, Sieberts SK, McCabe C, Patrick E, Xu J, Yu L, Gaiteri C, Bennett DA, Mostafavi S, De Jager PL. 2017. An xQTL map integrates the genetic architecture of the human brain's transcriptome and epigenome. *Nat Neurosci* **20**:1418–1426.

Ongen H, Buil A, Brown AA, Dermitzakis ET, Delaneau O. 2016. Fast and efficient QTL mapper for thousands of molecular phenotypes. *Bioinformatics* **32**:1479–1485.

Panopoulos AD, D'Antonio M, Benaglio P, Williams R, Hashem SI, Schuldt BM, DeBoever C, Arias AD, Garcia M, Nelson BC, Harismendy O, Jakubosky DA, Donovan MKR, Greenwald WW, Farnam K, Cook M, Borja V, Miller CA, Grinstein JD, Drees F, Okubo J, Diffenderfer KE, Hishida Y, Modesto V, Dargitz CT, Feiring R, Zhao C, Aguirre A, McGarry TJ, Matsui H, Li H, Reyna J, Rao F, O'Connor DT, Yeo GW, Evans SM, Chi NC, Jepsen K, Nariai N, Müller F-J, Goldstein LSB, Izpisua Belmonte JC, Adler E, Loring JF, Berggren WT, D'Antonio-Chronowska A, Smith EN, Frazer KA. 2017. iPSCORE: A Resource of 222 iPSC Lines Enabling Functional Characterization of Genetic Variation across a Variety of Cell Types. *Stem Cell Reports* **8**:1086–1100.

Pashos EE, Park Y, Wang X, Raghavan A, Yang W, Abbey D, Peters DT, Arbelaez J, Hernandez M, Kuperwasser N, Li W, Lian Z, Liu Y, Lv W, Lytle-Gabbin SL, Marchadier DH, Rogov P, Shi J, Slovik KJ, Stylianou IM, Wang L, Yan R, Zhang X, Kathiresan S, Duncan SA, Mikkelsen TS, Morrisey EE, Rader DJ, Brown CD, Musunuru K. 2017. Large, Diverse Population Cohorts of hiPSCs and Derived Hepatocyte-like Cells Reveal Functional Genetic Variation at Blood Lipid-Associated Loci. *Cell Stem Cell* **20**:558–570.e10.

Patro R, Duggal G, Love MI, Irizarry RA, Kingsford C. 2017. Salmon provides fast and bias-aware quantification of transcript expression. *Nat Methods* **14**:417–419.

Peng S, Deyssenroth MA, Di Narzo AF, Cheng H, Zhang Z, Lambertini L, Ruusalepp A, Kovacic JC, Bjorkegren JLM, Marsit CJ, Chen J, Hao K. 2018. Genetic regulation of the placental transcriptome underlies birth weight and risk of childhood obesity. *PLoS Genet*

14:e1007799.

Pertea G, Pertea M. 2020. GFF Utilities: GffRead and GffCompare. *F1000Res* **9**. doi:10.12688/f1000research.23297.2

Quach H, Rotival M, Pothlichet J, Loh Y-HE, Dannemann M, Zidane N, Laval G, Patin E, Harmant C, Lopez M, Deschamps M, Naffakh N, Duffy D, Coen A, Leroux-Roels G, Clément F, Boland A, Deleuze J-F, Kelso J, Albert ML, Quintana-Murci L. 2016. Genetic Adaptation and Neandertal Admixture Shaped the Immune System of Human Populations. *Cell* **167**:643–656.e17.

Quinlan AR, Hall IM. 2010. BEDTools: a flexible suite of utilities for comparing genomic features. *Bioinformatics* **26**:841–842.

Ramírez F, Ryan DP, Grüning B, Bhardwaj V, Kilpert F, Richter AS, Heyne S, Dündar F, Manke T. 2016. deepTools2: a next generation web server for deep-sequencing data analysis. *Nucleic Acids Res* **44**:W160–5.

Rubinacci S, Ribeiro DM, Hofmeister RJ, Delaneau O. 2021. Efficient phasing and imputation of low-coverage sequencing data using large reference panels. *Nat Genet* **53**:120–126.

Schmiedel BJ, Singh D, Madrigal A, Valdovino-Gonzalez AG, White BM, Zapardiel-Gonzalo J, Ha B, Altay G, Greenbaum JA, McVicker G, Seumois G, Rao A, Kronenberg M, Peters B, Vijayanand P. 2018. Impact of Genetic Polymorphisms on Human Immune Cell Gene Expression. *Cell* **175**:1701–1715.e16.

Schwartzentruber J, Foskolou S, Kilpinen H, Rodrigues J, Alasoo K, Knights AJ, Patel M, Goncalves A, Ferreira R, Benn CL, Wilbrey A, Bictash M, Impey E, Cao L, Lainez S, Loucif AJ, Whiting PJ, Gutteridge A, Gaffney DJ, HIPSCI Consortium. 2018. Molecular and functional variation in iPSC-derived sensory neurons. *Nat Genet* **50**:54–61.

Steinberg J, Southam L, Roumeliotis TI, Clark MJ, Jayasuriya RL, Swift D, Shah KM, Butterfield NC, Brooks RA, McCaskie AW, Bassett JHD, Williams GR, Choudhary JS, Wilkinson JM, Zeggini E. 2021. A molecular quantitative trait locus map for osteoarthritis. *Nat Commun* **12**:1309.

Taylor DL, Jackson AU, Narisu N, Hemani G, Erdos MR, Chines PS, Swift A, Idol J, Didion JP, Welch RP, Kinnunen L, Saramies J, Lakka TA, Laakso M, Tuomilehto J, Parker SCJ, Koistinen HA, Davey Smith G, Boehnke M, Scott LJ, Birney E, Collins FS. 2019. Integrative analysis of gene expression, DNA methylation, physiological traits, and genetic variation in human skeletal muscle. *Proc Natl Acad Sci U S A* **116**:10883–10888.

The GTEx Consortium. 2020. The GTEx Consortium atlas of genetic regulatory effects across human tissues. *Science* **369**:1318–1330.

Theusch E, Chen Y-DI, Rotter JI, Krauss RM, Medina MW. 2020. Genetic variants modulate gene expression statin response in human lymphoblastoid cell lines. *BMC Genomics* **21**:555.

van de Bunt M, Manning Fox JE, Dai X, Barrett A, Grey C, Li L, Bennett AJ, Johnson PR, Rajotte RV, Gaulton KJ, Dermitzakis ET, MacDonald PE, McCarthy MI, Gloyn AL. 2015. Transcript Expression Data from Human Islets Links Regulatory Signals from Genome-Wide Association Studies for Type 2 Diabetes and Glycemic Traits to Their Downstream Effectors. *PLoS Genet* **11**:e1005694.

van de Geijn B, McVicker G, Gilad Y, Pritchard JK. 2015. WASP: allele-specific software for robust molecular quantitative trait locus discovery. *Nat Methods* **12**:1061–1063.

Vija A, Alasoo K. 2022. Improved detection of genetic effects on promoter usage with augmented transcript annotations. *bioRxiv*. doi:10.1101/2022.07.12.499800

Wallace C. 2021. A more accurate method for colocalisation analysis allowing for multiple causal variants. *PLoS Genet* **17**:e1009440.

Wang G, Sarkar A, Carbonetto P, Stephens M. 2020. A simple new approach to variable selection in regression, with application to genetic fine mapping. *J R Stat Soc Series B Stat Methodol* **82**:1273–1300.

Wickham H. 2016. Data Analysis In: Wickham H, editor. ggplot2: Elegant Graphics for Data Analysis. Cham: Springer International Publishing. pp. 189–201.

Wilke CO. 2019. cowplot: streamlined plot theme and plot annotations for “ggplot2”. R package version 1.0. 0.

Yoon OK, Hsu TY, Im JH, Brem RB. 2012. Genetics and regulatory impact of alternative polyadenylation in human B-lymphoblastoid cells. *PLoS Genet* **8**:e1002882.

Young AMH, Kumasaka N, Calvert F, Hammond TR, Knights A, Panousis N, Park JS, Schwartzentruber J, Liu J, Kundu K, Segel M, Murphy NA, McMurran CE, Bulstrode H, Correia J, Budohoski KP, Joannides A, Guilfoyle MR, Trivedi R, Kirollos R, Morris R, Garnett MR, Timofeev I, Jalloh I, Holland K, Mannion R, Mair R, Watts C, Price SJ, Kirkpatrick PJ, Santarius T, Mountjoy E, Ghoussaini M, Soranzo N, Bayraktar OA, Stevens B, Hutchinson PJ, Franklin RJM, Gaffney DJ. 2021. A map of transcriptional heterogeneity and regulatory variation in human microglia. *Nat Genet* **53**:861–868.

Zeng T, Li YI. 2022. Predicting RNA splicing from DNA sequence using Pangolin. *Genome Biol* **23**:103.

Zhan X, Liu DJ. 2015. SEQMINER: An R-package to facilitate the functional interpretation of sequence-based associations. *Genet Epidemiol* **39**:619–623.

Zhao H, Sun Z, Wang J, Huang H, Kocher J-P, Wang L. 2014. CrossMap: a versatile tool for coordinate conversion between genome assemblies. *Bioinformatics* **30**:1006–1007.